Niche theory for mutualism:

A graphical approach to plant-pollinator network dynamics

Fernanda S. Valdovinos[1,*]

Robert Marsland III[2]

February 11, 2020

1. University of Michigan, Ann Arbor, Michigan 48109;

2. Boston University, Boston, Massachusetts 02215;

∗ Corresponding author; e-mail: fsvaldov@umich.edu.

The authors wish to be identified by the reviewers.

Manuscript elements: Figure 1, figure 2, figure 3, figure 4, figure 5, figure 6, figure 7, figure 8, figure 9, table 1, online appendices A, B and C including figure A1.

Keywords: Mutualism, niche theory, community ecology

Manuscript type: Article.

Abstract

Contemporary niche theory is a powerful framework for understanding how organisms interact with each other and with their shared environment. The graphical representation of the theory, as popularized by Tilman, facilitates the analysis of the equilibrium structure of complex dynamical models including species coexistence. This approach has so far been applied primarily to situations of resource competition, in accord with the general focus of work on ecological interactions since the 1970's. In this manuscript, we expand contemporary niche theory to integrate mutualistic interactions through a systematic analysis of mutualistic plant-pollinator networks. Specifically, we investigate the dynamics of a consumer-resource model of plant-pollinator interactions that has been extensively studied in numerical simulations and whose predictions have been tested against field data. We provide simple explanations in graphical terms for the qualitative phenomena consistently found by extensive numerical simulations, including the effects of nestedness and adaptive foraging on community dynamics, and the effects of invasions by new pollinator species. We also use this representation to highlight general similarities and differences between mutualistic systems and the more well-studied scenarios of pure competition.

Introduction

Mutualistic interactions pervade every type of ecosystem and level of organization on Earth (Boucher et al. 1982; Bronstein 2015). For example, mutualisms such as pollination (Ollerton et al. 2011), seed dispersal (Wang and Smith 2002), coral symbioses (Rowan 2004), and nitrogen-fixing associations between plants and legumes, bacteria, or fungi (Horton and Bruns 2001; van der Heijden et al. 2008) sustain the productivity and biodiversity of most ecosystems on the planet. Moreover, plant-pollinator mutualisms sustain human food security (Potts et al. 2016; Ollerton 2017) with one third of crop production relying on animal pollination. Despite their pervasiveness and critical role in ecological systems, ecological theory on mutualisms has been scarce and less integrated than for predation and competition (Vandermeer and Boucher 1978; Bascompte and Jordano 2014; Bronstein 2015). This scarce theoretical development is of particular concern because several mutualisms such as coral-algae and plant-pollinator that play a critical role in the functioning of ecosystems are currently under threat (Brown 1997; Rowan 2004; Goulson et al. 2015; Ollerton 2017). Thus, the absence of an integrated body of theory on the ecology of mutualism hinders our ability to protect, manage, and restore mutualistic systems. In particular, Niche Theory (MacArthur 1969, 1970; Tilman 1982; Leibold 1995; Chase and Leibold 2003) for mutualisms has only recently started to be developed (Peay 2016; Johnson and Bronstein 2019). Chase and Leibold (2003) suggest that their graphical approach can be expanded to mutualism, but such suggestions have yet to be fully explored. Here, we contribute to the development of ecological theory on mutualism by expanding Contemporary Niche Theory to mutualistic networks of plant-pollinator interactions. More specifically, we expand the graphical approach popularized by Tilman (1982) by applying it to a consumer-resource dynamic model of plant-pollinator networks developed and tested by Valdovinos et al. (2013, 2016, 2018).

For about 70 years, theoretical research analyzing the population dynamics of mutualisms roughly only assumed Lotka-Volterra type models (sensu Valdovinos 2019) to conduct their studies (Kostitzin 1934; Gause and Witt 1935; Vandermeer and Boucher 1978; Wolin and Lawlor 1984;

Bascompte et al. 2006; Okuyama and Holland 2008; Bastolla et al. 2009). Those models represent mutualistic relationships as net positive effects between species using a (linear or saturating) positive term in the growth equation of each mutualist that depends on the population size of its mutualistic partner. While this research increased our understanding of the effects of facultative, obligate, linear, and saturating mutualisms on the long-term stability of mutualistic systems, more sophisticated understanding of their dynamics (e.g., transients) and of phenomena beyond the simplistic assumptions of the Lotka-Volterra type models was extremely scarce. This lack of more sophisticated and mechanistic understanding of the dynamics of mutualistic interactions hindered conceptual (Bronstein 2015) and theoretical (Boucher 1985) progress on mutualistic interactions. In particular, key processes ignored by phenomenologically assuming positive net effects between mutualists are feeding and reproductive mechanisms that determine how direct interactions between mutualistic partners vary through time and across population densities or total abundances of the interacting species (Abrams 1987; Holland and DeAngelis 2010; Valdovinos et al. 2013).

A more mechanistic alternative to the Lotka-Volterra type models is the consumer-resource approach to mutualisms that was first proposed by Holland and colleagues (Holland et al. 2005; Holland and DeAngelis 2010) and further developed by Valdovinos et al. (2013, 2016, 2018). This approach decomposes the net effects assumed always positive by Lotka-Volterra type models (Fig. 1A) into the biological mechanisms producing those effects (i.e., the gathering of resources and exchange of services). The key advance of Valdovinos et al.'s model is separating the dynamics of the plants' vegetative biomass from the dynamics of the plants' floral rewards (e.g., nectar, Fig. 1B). This separation allows: i) tracking the depletion of floral rewards by pollinator consumption, ii) evaluating exploitative competition among pollinator species consuming the floral rewards provided by the same plant species, and iii) incorporating the capability of pollinators (adaptive foraging) to behaviorally increase their foraging effort on the plant species in their diet with more floral rewards available. Another advance of this model is incorporating the dilution of conspecific pollen carried by pollinators, which allows tracking competition among

plant species for the quality of pollinator visits. That is, this model assumes that pollinators visiting many different plant species carry more diluted pollen (low quality visits) than the pollen carried by pollinators visiting only one plant species (high quality visits). The incorporation of these biological mechanisms into a dynamic model of plant-pollinator networks enhances our understanding and predictive ability of the dynamics of species-rich mutualistic systems. For example, this model predicts that in networks with empirically observed structures (nested and moderately connected), pollinators with adaptive foraging will prefer on a per-capita basis plant species that interact with fewer pollinator species (i.e., specialist plants). Valdovinos et al. (2016) successfully tested this prediction with the distribution of per-capita foraging preferences of bumblebee species for their mutualistic plants in a montane ecosystem in Colorado. Moreover, the mechanisms incorporated in this model have provided insights into the process of species invasions, showing how species traits and network structure can predict the invasion success of alien pollinators and their impact on native species in computer-simulated plant-pollinator networks (Valdovinos et al. 2018).

In this contribution, we expand the graphical approach of the Contemporary Niche Theory (Chase and Leibold 2003) to analyze the dynamics of plant-pollinator networks when all the above-mentioned biological mechanisms are considered. More specifically, the present work – for the first time – analytically proves the results found with extensive numerical simulations (Valdovinos et al. 2013, 2016, 2018, hereafter "previous numerical simulations"), and generalizes some of them beyond the original simulation conditions. By "analytically proving" we refer to finding those results using a graphical approach whose geometry rigorously reflects mathematical analysis (Tilman 1982; Koffel et al. 2016) that can also be found in our Appendices. By developing and analyzing this graphical approach, we also expand Niche Theory to incorporate plant-pollinator networks, nestedness, adaptive foraging, quality of visits, and species invasions.

We start by describing Valdovinos et al.'s model and presenting our graphical approach to the dynamics of plant-pollinator mutualisms, which we present as our methods. Our first result is demonstrating that by modeling pollinators as obligate mutualists of plants (i.e., they depend

on floral rewards to survive) in a two trophic level system (i.e., plant and pollinator species without predators), the growth rate of pollinators is fully determined by the reward abundances and, therefore, the studied model falls within the niche theory framework and is subject to competitive exclusion. This means that at most the same number of pollinator as plant species can coexist at equilibrium regardless of the details of the dynamics. The first subsection of our results extensively explores and demonstrates the different conditions for coexistence among pollinator species motivated by the fact that empirical plant-pollinator networks typically exhibit twice to four times more pollinator than plant species (Vázquez et al. 2009). The second subsection of our results demonstrates the conditions for plant coexistence based on the relation between the strength of intra- and inter-specific competition among plants. This separate set of results reflects the biggest difference in population dynamics between pollinator and plant species in Valdovinos et al.'s model, that is, pollinator dynamics fully depend on floral rewards while plant dynamics also depend on other factors (space, light, nutrients) that are encapsulated within the model by a generic competition function composed of intra- and inter-specific competition coefficients that affect the recruitment rate of plants and are independent of the mutualistic interaction with pollinators (see Methods). The third subsection of our results demonstrates the effects on network dynamics of nestedness, that is, the tendency of generalists (species with many interactions) to interact with both generalists and specialists (species with one or a few interactions) and of specialists to only interact with generalists (Fig. 1c,d). This subsection analytically proves the results found by previous numerical simulations in nested networks without adaptive foraging (Valdovinos et al. 2013, 2016), that is, specialist species tend to go extinct due to high niche overlap among pollinators for floral rewards (Fig. 1c) and high niche overlap among plants for pollination services (Fig. 1d). The fourth subsection of our results demonstrates analytically the effects of adaptive foraging on network dynamics also found by previous numerical simulations (Valdovinos et al. 2013, 2016). These results consisted of adaptive foraging promoting species coexistence by allowing generalist pollinator species to focus their foraging efforts on specialist plant species (Fig. 2b) which releases floral rewards of generalist plants that can then

be consumed by specialist pollinators (compare red bars of Fig. 2a with 2b), and increases the visit quality for specialist plants. The fifth and final subsection of our results demonstrates the impacts of pollinator invasions on native pollinators found by previous numerical simulations (Valdovinos et al. 2018).

Overall, our work helps to integrate mutualistic interactions into Niche Theory, building off Peay (2016) who eloquently stated, "The niche is a central concept in ecology, and better integration of mutualism will more accurately reflect the positive interactions experienced by nearly all species."

Methods

Dynamical model of plant-pollinator interactions

The model of Valdovinos et al. (2013) separates the dynamics of the plants' vegetative biomass from the dynamics of the plants' rewards for each plant population (Fig. 1b). This separation allows tracking the depletion of rewards by animal consumption (indicated by 'Rewards consumption' in Fig. 1b) separately from the animal contribution to plants' population via pollination services (indicated by 'Pollination' in Fig. 1b). The vegetative growth and the floral-rewards dynamics of each plant population i are modeled separately as:

$$\frac{dp_i}{dt} = \gamma_i \sum_{j \in A_i} e_{ij}\sigma_{ij}(p_k)V_{ij}(p_i, a_j) - \mu_i^P p_i \tag{1}$$

$$\frac{dR_i}{dt} = \beta_i p_i - \phi_i R_i - \sum_{j \in A_i} V_{ij}(p_i, a_j) f_{ij}(R_i, p_i). \tag{2}$$

where $V_{ij} = \alpha_{ij}\tau_{ij}a_j p_i$ defines the frequency of visits by animal species j to plant species i, which increases the population growth of plant i (Eq. 1., 'Pollination' in Fig. 1b) but decreases its floral rewards (Eq. 2, 'Rewards consumption' in Fig. 1b). Note that R_i refers to the total amount of floral rewards the entire plant population i has avaialble for pollinator consumption. Pollinator visits are determined by the adaptive preference (thickness of pollinator's arrows in Fig. 1b) of animal j for rewards of plant i (α_{ij}, see below), the pollinator's visitation efficiency on plant i (τ_{ij})

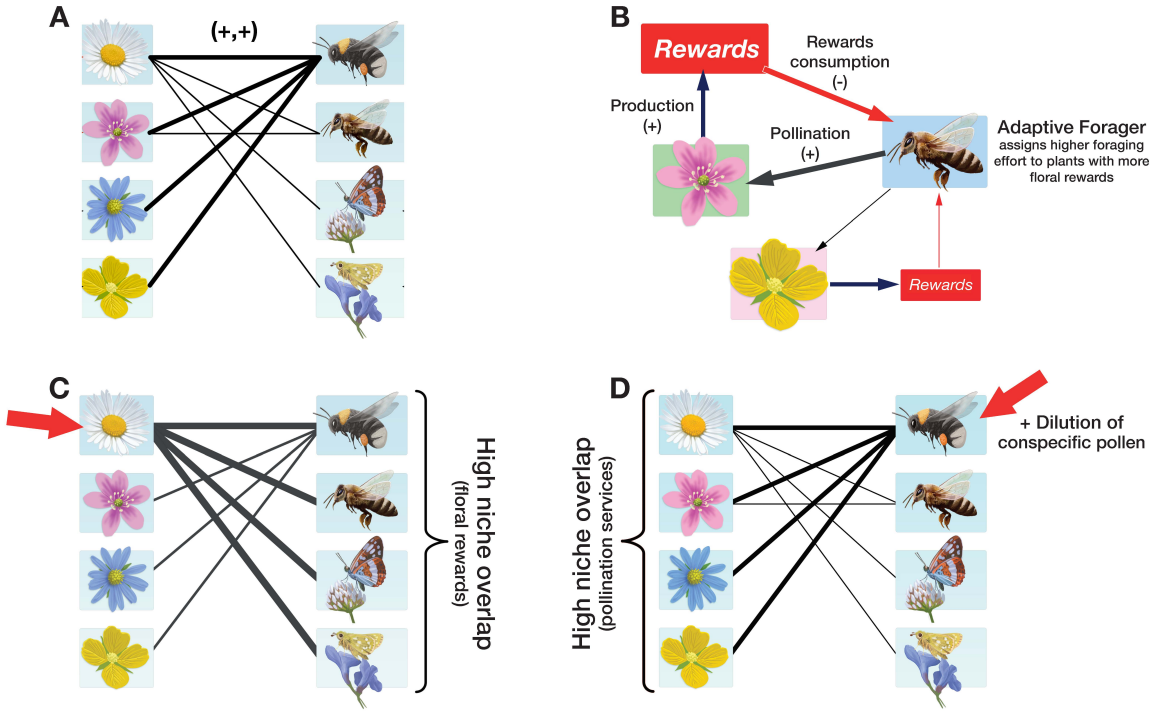

Figure 1: **Lotka-Volterra versus mechanistic modeling of mutualisms.** Illustration of Lotka-Volterra type (a) and Valdovinos et al.'s consumer-resource (b) models. (a) Key assumption of Lotka-Volterra type models is that mutualist partners always positively affect each other. (b) How Valdovinos et al.'s model decomposes net effects of mutualisms into two key mechanisms: consumption of floral rewards (indicated by 'Rewards consumption') and pollination services (indicated by 'Pollination'). The model separates the dynamics of the plant vegetative biomass (Eq. 1) from the dynamics of floral rewards (red rectangles, Eq. 2), connecting them by the plant production of rewards (indicated by 'Production', parameter β_i of Eq. 2). Adaptive foraging (Eq. 3) allows pollinators to assign higher foraging effort (thicker arrow) to plant species with higher floral rewards (larger rectangle). (c) High niche overlap among pollinator species that share floral rewards (follow thicker lines) of the most generalist plant species (indicated by the red arrow) in a nested network. (d) High niche overlap among plant species that share pollination services (follow thicker lines) of the most generalist pollinator species (indicated by the red arrow) in a nested network. This model also considers the dilution of conspecific pollen in the body of generalist pollinators (see function σ_{ij} in Eq. 1). Adapted from Valdovinos (2019) with permission.

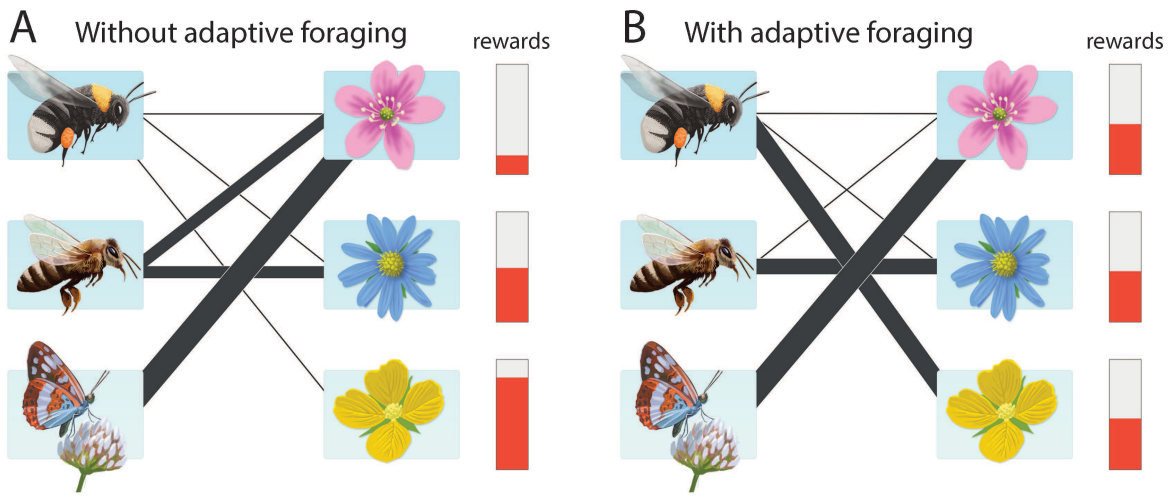

Figure 2: **Results of Valdovinos et al.'s model for nested networks.** (a) Without adaptive foraging, pollinator species partition the same foraging effort to each of their plant species (determined by Eq. 5 and illustrated by the width of the lines for each pollinator species), which results in generalist plant species (top right) receiving more visits than specialists (bottom right). This results in generalist plants having lower floral rewards than specialists do (red bars). In this scenario, specialist plant and animal species can go extinct because specialist plants receive very few and low quality visits while specialist pollinators have access to very low floral rewards and starve. (b) With adaptive foraging, generalist pollinator species (top left) partition higher foraging effort on specialist plant species (bottom right, follow thick line) which releases the rewards of generalist plant species now consumed by the specialist pollinators. In this scenario, specialist species persist because specialist plants receive more and higher quality of visits by generalist pollinators and specialist pollinators have enough food to persist. Reproduced from Valdovinos (2019) with permission.

and the population densities of animal j (a_j) and plant i (p_i). The sums are taken over the set A_i of pollinator species that are capable of visiting plant i.

In Eq. (1), only a fraction $\sigma_{ij} = \frac{\alpha_{ij}\tau_{ij}p_i}{\sum_{k\in P_j}\alpha_{kj}\tau_{kj}p_k}$ of j's visits successfully pollinate plant i, which accounts for dilution of plant i's pollen when j visits other plant species (indicated by the red arrow in Fig. 1B). A fraction e_{ij} of those pollination events produce seeds. Among those seeds, a fraction $\gamma_i = g_i(1 - \sum_{l\neq i\in P} u_l p_l - w_i p_i)$ recruit to adults, where g_i is the maximum fraction of i-recruits subjected to both inter-specific (u_l) and intra-specific (w_i) competition.

The population dynamics of animal j are defined as:

$$\frac{da_j}{dt} = \sum_{i\in P_j} c_{ij}V_{ij}(p_i, a_j)f_{ij}(R_i, p_i) - \mu_j^A a_j \tag{3}$$

where c_{ij} represents the per-capita efficiency of j converting plant i's floral resources into j's births. $f_{ij} = b_{ij}\frac{R_i}{p_i}$ is the quantity of nectar extracted per visit, where b_{ij} represents the efficiency of j extracting plant i's floral resources (R_i, Eq. 2). The sum is taken over the set of plant species P_j that can be visited by pollinator j. The visit frequency V_{ij} and the quantity of nectar extracted can also both be modeled by a saturating function following Holling's Type II functional response (Holling 1959), as discussed in Appendix A.

Another key advance of this model accounts for the widely observed adaptive foraging of pollinators (Fig. 1B) by modeling the adaptation of animal j's foraging preference on i as:

$$\frac{d\alpha_{ij}}{dt} = G_j\alpha_{ij}\left(c_{ij}\tau_{ij}b_{ij}R_i - \sum_{k\in P_j}\alpha_{kj}c_{kj}\tau_{kj}b_{kj}R_k\right) \tag{4}$$

with $\sum_{k\in P_j}\alpha_{kj} = 1$. The preference α_{ij} increases when the rewards that could be extracted from plant species i by application of full foraging effort to that plant ($\alpha_{ij} = 1$) exceed the rewards currently obtained from all plants in j's diet (follow thicker pollinator's arrow in Fig. 1B). The preference decreases in the opposite case, where the rewards obtainable by exclusive foraging on plant i are lower than the current rewards uptake level. When adaptive foraging is not considered, foraging efforts of pollinator species j are fixed to

$$\alpha_{ij} = \frac{1}{P_j} \tag{5}$$

where P_j here represents the number of plant species visited by pollinator species j.

Niche theory for plant-pollinator dynamics

The concept of a "niche" has long been central to ecological theory. Over the past fifty years, this concept has been significantly clarified and refined, beginning with the pioneering work of Levins, MacArthur and Tilman, and more recently consolidated by Chase and Leibold (MacArthur 1969, 1970; Tilman 1982; Leibold 1995; Chase and Leibold 2003). This framework highlights two distinct aspects of an organism's niche: its requirements for survival and its impact on the environment (Leibold 1995). The state of the environment is mathematically represented by a vector in an abstract space, whose components correspond to concentrations of resources, populations of predators, stress intensity, or any other factors that affect an organism's growth rate (Levin 1970). Here, we analyze the niche of plant and pollinator species within their mutualistic interactions, assuming all their other niche variables (e.g., soil nutrients, water, temperature, nesting sites) constant and sufficient for supporting their populations.

For plant-pollinator systems, there are two reasonable choices for the definition of the environment space. On short time scales, such as within a single flowering season, the plant populations can be regarded as constant, and the relevant environmental factors are the floral rewards R_i, as shown in Fig. 3*(a)*. On longer time scales, one can use the plant populations p_i as the axes for the environment space, as in Fig. 3*(b)*, letting the reward levels implicitly determine the value of each plant population as a food source. Table 1 summarizes both representations in terms of the model parameters.

In either space, the "requirement niche" of each animal species j ($j = 1, 2 \ldots A$) can be encoded by a zero-net-growth isocline (ZNGI) (Tilman 1982; Leibold 1995). The ZNGI is a hypersurface that separates the environmental states where the growth rate g_j is positive from the states where it is negative. Environmental states along the ZNGI support reproduction rates that exactly balance mortality rates, leading to constant population sizes. The ZNGI thus represents one boundary of Hutchinson's "fundamental niche," which is the hypervolume of environmental

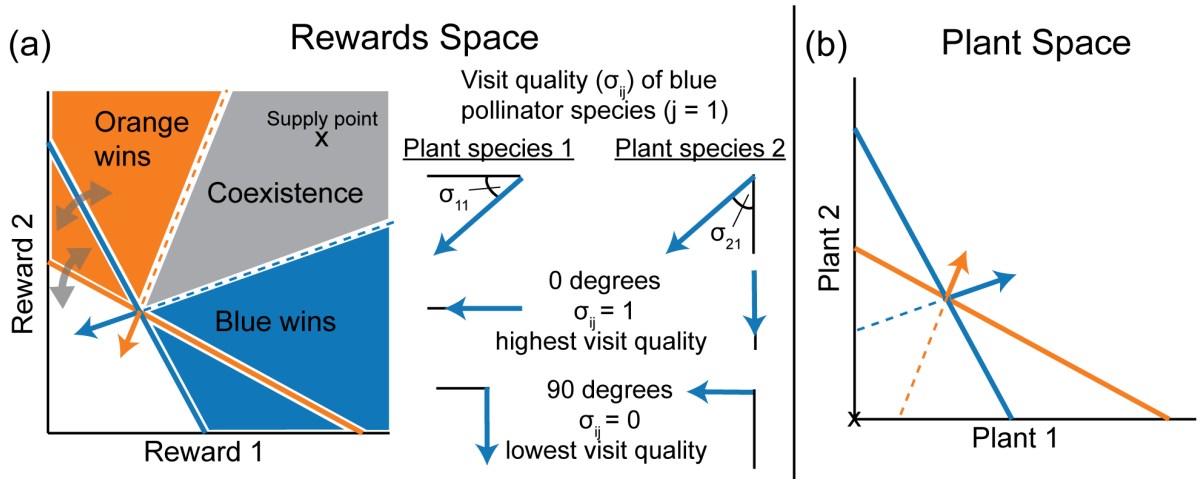

Figure 3: **Niche theory for mutualism.** *(a)* Representation of plant-pollinator system as a standard consumer-resource type model, for time scales on which plant populations are approximately constant. For each pollinator (blue or orange) the *impact vector* (colored arrow) encodes per-capita consumption rates of rewards by the pollinator, while the *zero net-growth isocline* (ZNGI, colored line) indicates the abundance levels of floral rewards at which the pollinator growth rate vanishes. The fate of each pollinator species at equilibrium is determined by the location of the *supply point* for the rewards, which depends on the population densities of the plant species. Both pollinator species stably coexist if the supply point lies in the gray "coexistence cone" bounded by the dotted lines extended backwards from the impact vectors. Adaptive foraging causes the ZNGIs and impact vectors to rotate in the direction of the most abundant resource. The angle between the impact vector and a given rewards axis affects the pollinator's visit quality for the corresponding plant, with zero degrees corresponding to $\sigma_{ij} = 1$ (highest visit quality), and 90 degrees corresponding to $\sigma_{ij} = 0$ (lowest visit quality). *(b)* Representation in terms of plant populations for analysis of longer time scales, where the mutualism becomes visible. The "supply point" is now located at the origin, and the pollinator impacts are necessary to sustain nonzero plant abundance. The location of the ZNGIs depends on the current nutritional value of each plant species, which is lower for species whose floral rewards are more depleted. The impact vectors depend on the visit quality and the per-capita visit frequency of each pollinator species (σ_{ij} and V_{ij}/a_j of Eq. 1, respectively), and encode each pollinator's contribution to the total number of seedlings in the next generation.

Rewards Space		
Niche concept	**Description**	**Mathematical expression**
ZNGI	Reproduction/mortality balance	$\sum_{i \in P_j} c_{ij}(V_{ij}/a_j) f_{ij} = \mu_j^A$
Impact Vector	Reward depletion	$-(V_{ij}/a_j) f_{ij}$
Supply Point	Reward production	$\beta_i p_i / \phi_i$
Plant Space		
Niche concept	**Description**	**Mathematical expression**
ZNGI	Reproduction/mortality balance	$\sum_{i \in P_j} c_{ij}(V_{ij}/a_j) f_{ij} = \mu_j^A$
Impact Vector	Plant production	$\gamma_i e_{ij} \sigma_{ij}(V_{ij}/a_j)$
"Supply Point"	Plant mortality	0

Table 1: Mapping elements of the model to niche theory concepts.

conditions in which the species can survive indefinitely (Hutchinson 1957; Leibold 1995; Chase and Leibold 2003). Adaptive foraging allows the ZNGIs in rewards space to dynamically rotate in the direction of the most abundant rewards. In plant space, the ZNGIs are dynamic even in the absence of adaptive foraging, because the contribution each plant makes to the growth rate depends on the current reward level R_i.

The "impact niche" is represented by an *impact vector*, which specifies the magnitude and direction of the environmental change induced by a single individual of the species (Tilman 1982; Leibold 1995). The impact vector thus encodes the "role" of an organism in the community, and roughly corresponds to Elton's niche concept (Elton 1927; Leibold 1995). In plant space, the mutualism is directly visible in the impact vector, which represents the number of successful pollination events caused by each pollinator, and points in the direction of larger plant population sizes. In rewards space, however, the impact of a pollinator species is simply the rate at which it depletes the floral rewards, just as in an ordinary model of resource competition. But the angle of the impact vector takes on a new importance, because it affects the visit quality σ_{ij}. If the impact vector is nearly perpendicular to a given rewards axis, this means that only a small fraction of its

visits are allocated to the corresponding plant, and so most of the pollen carried by this pollinator belongs to other plant species. If all of the visits received by this plant species have such low quality, the plant may eventually go extinct, as we will see below.

The environment also has its own intrinsic dynamics, represented by a *supply vector* (Tilman 1982; Chase and Leibold 2003). In plant space, there is no "supply" apart from the seed production mediated by the pollinators, with the result that the "supply vector" is directed towards the origin. In rewards space, the supply vector points towards the *supply point* where the rewards reach equilibrium in the absence of pollinators, as it would in an ordinary niche theory model. But the supply point itself is determined by the plant populations, which depend on pollination activity for their long-term survival. Extinction of a plant species (e.g., due to low visit quality) causes the supply point to drop to zero along the corresponding rewards axis, leading to a cascade of ecological reorganization.

These three quantities (ZNGIs, impact vectors, and supply point) define the conditions for stable coexistence, which can be represented graphically in the case of two plant species $P = 2$, as illustrated in Fig. 3. From the definition of the ZNGI, it follows that nonzero animal populations can only be in equilibrium when all the corresponding ZNGIs pass through the current environmental state. But for the environment to remain in this state, the combined impact of the pollinators must exactly cancel the supply. This total impact is found by multiplying each impact vector by the corresponding population density, and then summing the results. Whenever the supply point lies within the cone formed by extending all the impact vectors backwards, as shown in Fig. 3, a set of population densities can be found with a total impact equal and opposite to the supply. Each potentially stable consortium of coexisting species is thus represented by an intersection of ZNGIs, and coexistence is achieved whenever the supply point falls within the corresponding coexistence cone. The relative population sizes required can be roughly estimated from the position of the supply point within the cone. If one of the impact vectors points almost directly away from the supply point, then only a small contribution will be required from the other pollinator species to achieve perfect cancellation of the supply.

Results

We use the graphical approach presented above to expand, qualitatively understand, and analytically prove the previously reported results of large-scale numerical experiments with this model (Valdovinos et al. 2013, 2016, 2018). In particular, we present: i) Conditions for coexistence among pollinator species, ii) conditions for coexistence among plant species, iii) effects of nestedness on network dynamics without adaptive foraging, iv) effects of adaptive foraging on network dynamics, and v) impacts of pollinator invasions on native species. We will use two-dimensional illustrations similar to Fig. 3, since higher dimensions cannot be easily visualized, but the qualitative results of interest hold for arbitrary P.

1. Conditions for coexistence among pollinator species

As noted above, the definition of the ZNGI implies that multiple species can potentially coexist at equilibrium only if their ZNGIs simultaneously intersect. If the ZNGIs fail to cross, the species cannot coexist, regardless of the details of the dynamics. For each pollinator species j, we can find the ZNGI in rewards space by setting $da_j/dt = 0$ in Eq. (3) for fixed reward abundances R_i. From the resulting formula, given in Table 1, and the fact that $\sum_{i \in P_j} \alpha_{ij} = 1$, it follows that the ZNGIs for all possible foraging strategies α_{ij} of pollinator species j intersect at the point in rewards space defined by

$$R_i^* = \frac{\mu_j^A}{c_{ij}\tau_{ij}b_{ij}}. \tag{6}$$

This is Tilman's "R^*" (Tilman 1982) for specialists on plant species i, that is, the minimal resource level that supports growth of the pollinator species. Whenever the reward abundances for all plant species are simultaneously found at this minimal level, all the species have equivalent value for pollinator species j, and the pollinator growth rate equals zero for any choice of foraging strategy.

Previous numerical simulations (Valdovinos et al. 2013, 2016, 2018) gave all species very sim-

ilar values for resource conversion (c_{ij}), foraging (τ_{ij}) and ingestion (b_{ij}) efficiencies, as well as for the mortality rate (μ_j^A) , so that the only differences between species were those resulting from the structure of the interaction network (i.e., the set of plants P_j that are included in the sum in Eq. 3). Typically, the interaction network constitutes the primary source of empirical data about a given plant-pollinator system, and so focusing the simulations on the effect of network structure is a reasonable choice. An important consequence of this assumption is that the above discussion of ZNGI's for different possible foraging strategies of a single pollinator species also applies across species. In particular, when these parameters are perfectly species-independent, then the R_i^* are also the same for all species in the community, as illustrated in Fig. 4*(a)*, opening up the possibility of universal coexistence, regardless of the number of plant species.

Despite the lack of empirical data to estimate the parameters of the different pollinator species mentioned above, there is empirical evidence suggesting that the net reward uptake efficiency ($c_{ij}\tau_{ij}b_{ij}$) and the mortality rate (μ_j^A) parameters should scale with the same power of body size (i.e., should scale allometrically, Yodzis and Innes 1992; Pacciani-Mori et al. 2019). Because the former appears in the denominator of Eq. (6) and latter in the numerator, the allometric scaling of these parameters results in similar values of R_i^* regardless of the variability in the individual parameters (Yodzis and Innes 1992; Pacciani-Mori et al. 2019).

But even a small difference in R_i^* between species can prevent ZNGIs from intersecting, which rules out stable coexistence. In fact, the graphical perspective shows conclusively that this model is subject to the Competitive Exclusion Principle (CEP), which states that the maximum number of coexisting consumers at equilibrium cannot exceed the number of distinct resource types – here, the number of plant species P. In Fig. 4*(a)*, with $P = 2$, it is easy to see that no more than two ZNGIs can intersect at the same point without infinitely precise fine-tuning. When $P = 3$, the ZNGIs become planes, and at most three of them can intersect simultaneously. This pattern extends to arbitrarily high dimension, as can be proven mathematically (Levin 1970; McGehee and Armstrong 1977). In fact, for any P, the ZNGI has dimension $P - 1$, and the CEP is simply the statement that at most P surfaces of dimension $P - 1$ can intersect in an P-dimensional space.

Empirical plant-pollinator networks, however, frequently exceed this bound with about 2-4 times more pollinator than plant species (Vázquez et al. 2009). A large body of literature (e.g., Hutchinson 1961; Richerson et al. 1970; Levin 1974; Levins 1979; Turner et al. 1996; Huisman and Weissing 1999; Kerr et al. 2002; Czárán et al. 2002; Kelsic et al. 2015; Xue and Goldenfeld 2017; Posfai et al. 2017) has found a variety of mechanisms for CEP violation, which increase diversity above this limit by either preventing the system from reaching equilibrium, or modifying the model in ways that render the ZNGI-based analysis inadequate. These reasons can also apply to both plants and animals within plant-pollinator networks. Here, we focus on a few of those mechanisms that are more directly applicable to the studied model: modifying the ZNGI's with direct self-limitation or predation, and avoiding equilibrium with long-lived transient dynamics.

Modifying ZNGI with direct self-limitation or predation

The simplest way to avoid competitive exclusion is to add a direct self-limitation term to the pollinator dynamics (e.g., in the denominator of the functional response with $\omega_{jj} > 0$ in Eq. A3 of Appendix A). An arbitrary number of species can coexist if each species is capable of detecting its own density, and of reducing its growth rate before resources are depleted to the minimum viable level (cf. Chesson 2000). Geometrically, direct self-limitation makes the ZNGIs depend on the pollinator abundances, generating a feedback mechanism that (under suitable environmental conditions) adjusts the ZNGIs until they exactly intersect.

Another way of allowing for more coexistence in the model is to incorporate other environmental factors in the growth rate of pollinators. One such factor is population loss due to predation. Each predator species adds another axis to the environmental space in which the ZNGIs are defined, and makes the coexistence of an additional species geometrically possible (Levin 1970; McGehee and Armstrong 1977; Leibold 1998). If one still focuses on the P-dimensional rewards subspace, it will appear that the ZNGIs are perfectly fine-tuned in such a way as to allow more than P of them to simultaneously intersect.

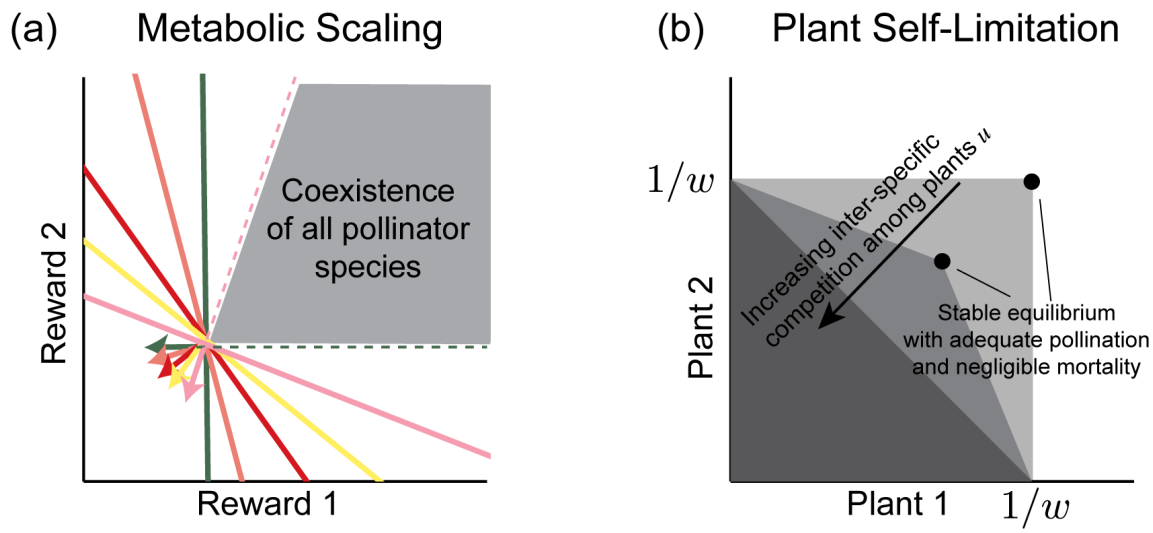

Figure 4: **Constraints on parameter values for allowing species coexistence.** *(a)* The competitive exclusion principle results from the geometric fact that no more than P ZNGIs (Zero Net Growth Isoclines) can generically intersect in an environmental space of P dimensions. In empirical plant-pollinator systems, however, the number of coexisting pollinator species can be twice to four times as large as the number of plant species. This suggests that other factors not explicitly included in the model force all the ZNGIs to nearly intersect at a single point in rewards space, so that the time scale for enforcement of competitive exclusion is much longer than the ecologically relevant time. In the main text we describe how metabolic theory can partially explain this constraint, which was achieved in previous numerical simulations by giving all pollinator species similar values of c_{ij}, τ_{ij}, b_{ij} and μ_j^A. *(b)* The shape of the region of plant space where equilibrium can be achieved depends on the relative strengths of intra- vs. inter-specific competition. This region is shaded in progressively darker shades of gray for increasing levels of uniform inter-specific competition $u_i = u$ and fixed intra-specific competition $w_i = w$. In the limit of small mortality (compared with low-density rate of seedling generation), the stable equilibrium state is near the outer corner of the box, as indicated by the black dots and shown in Appendix B. When the strength of inter-specifc and intra-specific competition become equal, however ($u = w$, see expression of the recruitment function γ_i in the main text), this corner vanishes, as does the state of stable coexistence. In the numerical experiments, the u_l were set to small values, corresponding to the lightest shaded region in the diagram.

Nonequilibrium properties and long-lived transients

Above, we noted that unlimited coexistence is possible with a finite set of plant species when the rewards uptake efficiency scales perfectly with pollinator mortality rates, giving all pollinator species the same set of minimal viable reward abundances R_i^*. If this scaling is not perfect, the timescale for enforcement of competitive exclusion can be easily estimated in terms of the generation time of the species of interest, using the relative deviations of the parameters from the scaling law. To see this, we first note that for any value of $c_{ij}\tau_{ij}b_{ij}$, there is a mortality rate μ_j^{A0} that exactly follows the scaling law, and would lead to stable coexistence. If species j is in fact destined to be excluded, this definition implies that its population dynamics during the final relaxation to equilibrium (with $R_i \approx R_i^*$) are described by $\frac{da_j}{dt} = -a_j\delta\mu_j$ where $\delta\mu_j = \mu_j^A - \mu_j^{A0}$. But μ_j^{A0} is also related to the generation time, since this is the mortality rate that would exactly balance the birth rate under the given environmental conditions. This means that the doubling time for species j in the absence of mortality is $T_j = \ln 2/\mu_j^{A0}$. We thus conclude that the number of generations (measured by doubling time) required for the population of the excluded species to drop by half is:

$$n_{\text{CEP}} = \frac{\ln 2}{T_j\delta\mu_j} = \frac{\mu_j^{A0}}{\delta\mu_j} \tag{7}$$

which is the inverse of the relative "error " in the mortality rate μ_j^A.

In the simulations reported in Valdovinos et al. (2013, 2016), $\delta\mu_j/\mu_j^{A0}$ was set to 0.01%, so that competitive exclusion would take 10,000 generations to set in, which is far longer than an ecologically relevant time-scale in plant-pollinator systems, where a generation usually corresponds to one flowering season. Since the reported simulation results come from runs of about 100 or 200 generations, which is a more ecologically pertinent time-scale, competitive exclusion was irrelevant.

Although studies of allometric scaling relationships (cf. Yodzis and Innes 1992) support the assumption of proportionality between mortality and mass-specific uptake, it is difficult to imagine a mechanism that would give this scaling a precision of less than ten percent. This means

that realistic competitive exclusion times would be less than 10 generations, so other mechanisms are still required to allow CEP violation over the long term.

In the graphical analysis presented here, we will follow previous numerical simulations, and assume that using identical R_i^* values for all species captures the community structure on ecologically relevant time scales.

2. Conditions for coexistence among plant species

Unlike the population growth rate of pollinators that entirely depends on rewards abundances, the population growth rate of plants in the Valdovinos et al. model considers other factors (e.g., space or nutrient limitation) that are captured by a generic function of plant competition composed of intra- (or self-limitation) and inter-specific competition coefficients (w_i and u_l, respectively) that affect plant recruitment rate (γ_i in Eq. A3) and are independent of the mutualistic interaction with pollinators. Therefore, determining conditions for potential coexistence among plant species is more straightforward than among pollinator species. The minimal requirement for plant population survival, in the ideal scenario of no plant mortality, is that the recruitment rate γ_i must be positive. We can therefore draw a Hutchinsonian niche for each plant species i as the set of combinations of plant densities p_k that give rise to a positive γ_i. We represent the intersection of the niches for a pair of plant species in Fig. 4*(b)*, where the shape and extent of the region of allowed equilibrium states for the plant abundances depends on the relative importance of intra- vs. inter-specific competition.

If each plant has its own independent niche, and is not directly affected by other species, then all species can coexist at equilibrium anywhere in the box bounded by the surfaces (or lines in two dimensions) $p_i = 1/w_i$. In the limit where the mortality rate is small compared to the rate of seedling generation at low plant density, plant populations take on the maximum allowed value, and the equilibrium is always near the outer corner of the box $p_i^* \approx 1/w_i$ for all i. As inter-specific competition increases, the far corner of the box is pulled towards the origin. In Appendix B, we show for the case of uniform coefficients ($w_i = w$ and $u_l = u$ for all i and l)

that a necessary condition for stable plant coexistence is that intra-specific competition should be stronger than inter-specific competition ($w > u$), in accordance with modern coexistence theory (Chesson 2000). Geometrically, this corresponds to the case where the shaded region in Fig. 4*(b)* remains convex.

To simplify our analysis, in the next subsections we will focus on the case of low inter-specific competition (i.e., $u_l \ll w_i$), which is also the regime where all the relevant numerical simulations were performed (Valdovinos et al. 2013, 2016, 2018), so we can safely approximate $p_i^* \approx 1/w_i$ under conditions of adequate pollination.

3. Effects of nestedness on network dynamics without adaptive foraging

Most empirical plant-pollinator networks exhibit a nested structure (Bascompte et al. 2003; Bascompte and Jordano 2007, definition provided in the Introduction). The implications of nestedness for the stability of these networks have been a topic of study for over a decade (Bastolla et al. 2009; Allesina and Tang 2012, reviewed in Valdovinos 2019). One of the first goals of the model studied here was to provide a more mechanistic framework to evaluate the effects of nestedness on the dynamics of plant-pollinator networks. The following summarizes the results and mechanistic explanation provided by the model and simulations in Valdovinos et al. (2013, 2016). Specialist species tend to go extinct or decline in abundance due to high niche overlap among pollinators for floral rewards (Fig. 1C) and high niche overlap among plants for pollination services (Fig. 1D). In nested networks, generalist pollinators visit generalist and specialist plants while specialists tend to visit only generalist plants and, therefore, specialist pollinators compete for the depleted rewards of generalist plants with generalist pollinators that have the advantage of getting resources (rewards of specialist plants) that are not shared with the specialist pollinators. Likewise, specialist plants in nested networks tend to receive visits only by generalist pollinators that carry more diluted pollen (lower visit quality), while generalist plants also receive visits by specialist pollinators that carry their conspecific pollen (higher visit quality). In this subsection, we analytically prove these results using our graphical approach and demonstrate novel ones

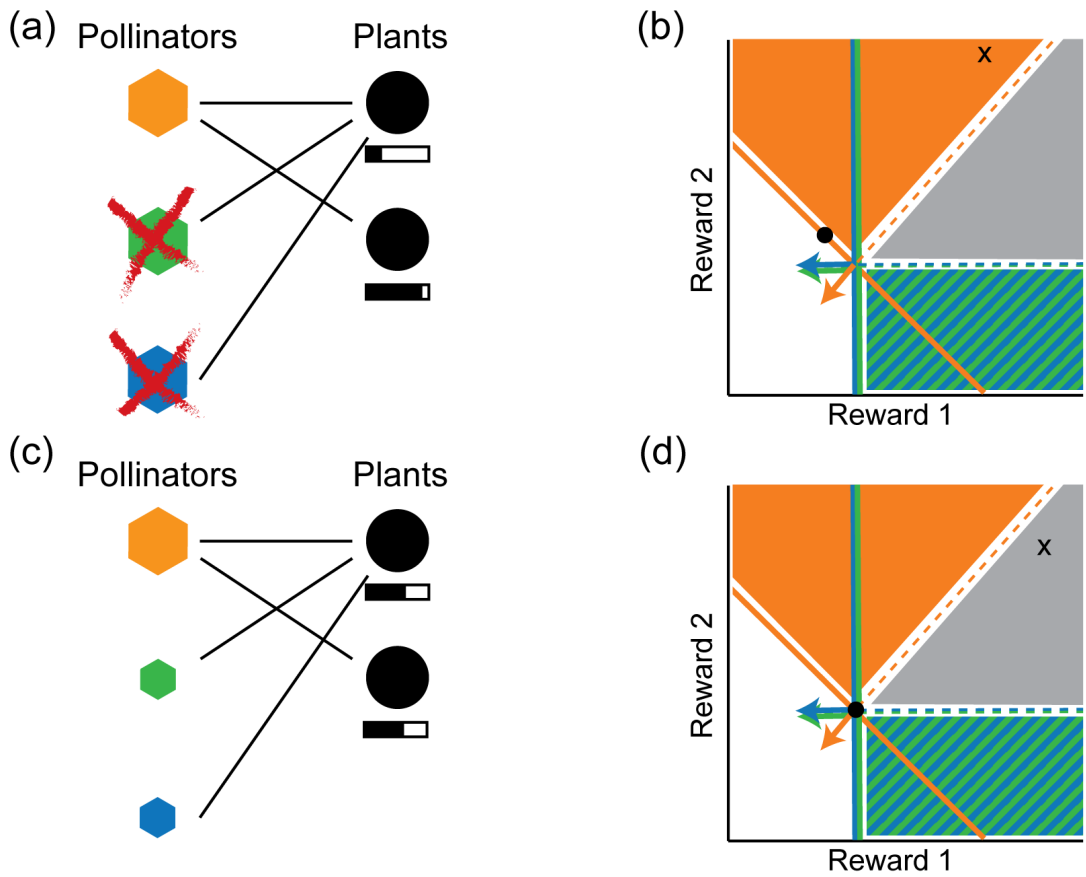

Figure 5: **Effects of nestedness on pollinators.** *(a)* Nested network with three pollinator species (polygons) and two plant species (circles). Shaded bar under each circle indicates abundance of available floral rewards, for scenario where plant species 2 has slightly higher abundance than plant species 1 ($\beta_2/w_2 > \beta_1/w_1$). Rewards levels correspond to the equilibrium point in panel b, with the difference between species exaggerated for clarity. *(b)* ZNGIs, impact vectors and supply point for the network in panel a. The fact that plant species 2 has slightly higher abundance implies that the supply point lies above the diagonal, outside the coexistence cone, so the two specialist species are driven to extinction. Final equilibrium reward levels are indicated by the black dot, with more available rewards from plant species 2 than from species 1, in agreement with schematic in first panel. *(c)* Same network, with rewards bars corresponding to the case where plant 1 has slightly higher abundance than plant 2 ($\beta_1/w_1 > \beta_2/w_2$). *(d)* Corresponding ZNGIs, impact vectors and supply point. Since plant 1 has higher abundance, the supply point lies slightly below the diagonal, within the coexistence cone. But since the impact vector of the generalist pollinator species points almost directly away from the supply point, this species almost maintains resource equilibrium on its own, and the population of specialist species required to cancel the remaining component of the rewards supply is small.

that were not found by previous work. In the following subsection, we analyze how these results are modified when adaptive foraging is included in the model.

We first analyze the pollinator side. Although the above mentioned results were obtained using numerical simulations with tens to hundreds of species, these qualitative results can be extracted from smaller systems for ease of visualization and interpretation of our graphical approach. In this entire work, we use a small nested network of three pollinator and two plant species illustrated in Fig. 5. The relationship between mortality and consumption rates presented in the first subsection of our results guarantees that all three ZNGIs pass through the same point (R_1^*, R_2^*) in the space of floral rewards, defined by the minimum viable reward levels for specialist animals. The supply point $(\beta_1 p_1, \beta_2 p_2)$ depends on the plant population sizes p_1 and p_2, which unveils the nature of mutualistic interactions within the niche theory framework. We first consider the case where both plants are highly productive, with low mortality, so that $p_i \approx 1/w_i$ as discussed in the previous section.

As noted above, previous simulation work focused on the effect of network structure on community dynamics, holding all other variables nearly fixed. Specifically, all model parameters other than the network structure (i.e., who interacts with whom) were obtained by adding small species-dependent random numbers to fixed species-independent values. For example, the plant self-limitation terms w_i were given by $w_i = w + \delta w_i$, where the δw_i were sampled from a uniform probability distribution over a small interval (compared to w) with mean zero. An immediate consequence of this sampling protocol is that the generalist impact vector points nearly along the diagonal away from the origin, and the supply point $(\beta_1/w_1, \beta_2/w_2)$ lies close to this same diagonal, as shown in Fig. 5.

With this setup we analyze the two possible results of this model found by previous numerical simulations, one corresponding to the generalist pollinators outcompeting the specialists and the second corresponding to the coexistence among pollinators where specialist species have much lower abundance than the generalists. The first result is illustrated in Fig. 5*(a)-(b)*, where the random contribution to w_i and β_i places the supply point just outside the coexistence cone, with

the specialist plant (species 2) providing a slightly higher reward supply than the generalist (species 1). In this case, the specialist plant species has higher rewards abundance at equilibrium than the generalist, and the specialist pollinator species go extinct due to starvation.

The second result is illustrated in Fig. 5*(c)*-*(d)*, where the supply point lies just inside the coexistence cone. All three pollinator species survive, but with the population size of the specialist species much lower than that of the generalist. Because the random contribution to the parameters is small, the impact vector of the generalist pollinator points almost directly away from the supply point, and so it is nearly capable of maintaining the rewards equilibrium on its own. Only a small contribution from the specialists is required to balance out the remaining component of the rewards supply. The equilibrium rewards abundance lies at the coexistence point (R_1^*, R_2^*), where the available rewards from both plants have equal value.

Analyzing the dynamics of plant species using our graphical approach reveals the key difference between the rewards space of mutualistic dynamics and an ordinary consumer-resource model, that is, that the supply point is maintained by the activity of the mutualistic partners (pollinators). This is most clearly visible in cases where pollinators fail to sufficiently supply the reproductive services of a plant species, and the plant species goes extinct. In nested networks, as illustrated in Fig. 6*(a)*, specialist plants are the most susceptible to extinction because they are typically pollinated only by generalist pollinators, which carry more diluted con-specific pollen (given that they visit different plant species, see Model description). We found a critical value of visit quality below which a plant species goes extinct, which was not found by previous simulation work. This novel result shows that, as long as the supply point remains in the coexistence cone, the quantity of visits V_{ij} of a pollinator species j to a pure specialist plant species i (visited only by pollinator j) can be written as a simple function of the plant abundance p_i alone. This allows us to obtain a simple formula for the plant population p_i as a function of the visit quality σ_{ij}, derived in Appendix C and illustrated in Fig. 6*(c)*.

Here, we further describe our novel result. In the regime where consumption by pollinators is the primary source of rewards depletion (rather than loss due to other causes encoded in the

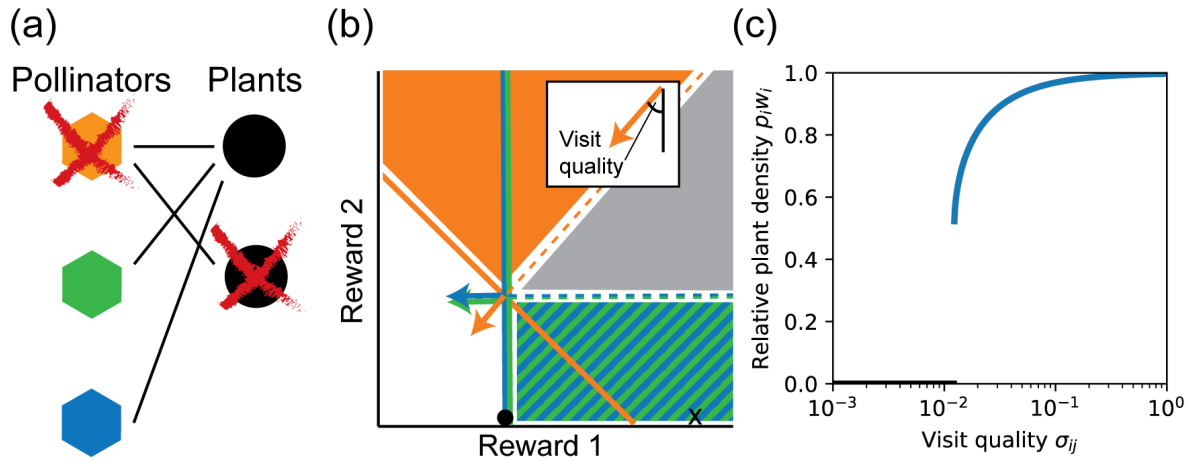

Figure 6: **Effects of nestedness on plants.** *(a)* Nested network with three pollinator species (polygons) and two plant species (circles). *(b)* Corresponding ZNGIs, impact vector and supply point, illustrating how the supply point drops to zero along the rewards axis of the specialist plant species if the visit quality σ_{21} of the generalist pollinator species to this plant is too low. With the specialist plant extinct, the generalist pollinator is outcompeted by the specialists, and also goes extinct. *(c)* Dependence of specialist plant population density p_i on visit quality σ_{ij}, using parameter set 'mu2' from Valdovinos et al. (2013), which corresponds to high mortality of plants and low mortality of pollinators. Plant population is measured in units of the plant's carrying capacity $1/w_i$. See Appendix C for derivation.

$\phi_i R_i$ term of Eq. 2), the formula yields a critical quality $\sigma_c \approx 4/s_{ij}$, where s_{ij} is the number of seedlings produced over the lifetime of an individual plant under optimal conditions of low plant density and no pollen dilution. When $\sigma_{ij} > \sigma_c$, the plant population is stable near its carrying capacity $p_i \approx \frac{1}{w_i}$, but as the quality crosses this threshold, the species suddenly goes extinct. In Fig. 6*(b)* we show how this extinction moves the supply point to zero along the rewards axis corresponding to the specialist plant species (i.e., plant and Rewards 2). The supply point now lies below the coexistence cone, so that only the specialist pollinator species survive, whereas only the generalist species survived before. This is because the generalist pollinators without adaptive foraging only assign half of their foraging effort to the persistent plant species (i.e, generalist plant species corresponding to plant and Rewards 1 in Fig. 6), while their other half is still assigned to the extinct plant species 2. Assigning only half of their foraging efforts to the persistent species places the generalist pollinators as inferior competitors with respect to the specialist pollinators that assign all their effort in extracting rewards of the persistent plant species (Valdovinos et al. 2016). This phenomenon of generalist pollinators assigning effort in searching for an extinct plant species in unlikely to happen in nature, but is a feature of the model when adaptive foraging is not considered. A more realistic version of the model (with adaptive foraging) is analyzed below, where this phenomenon does not occur.

This result of specialist pollinators surviving and generalists going extinct without adaptive foraging provides an example of how different species of pollinators can help each other through shared plant species, even when they compete for these plants' floral rewards. The extinction of plant species 2 and consequent loss of the generalist pollinator species was caused by the low quality of visits to this plant. If a new pollinator species specializing on plant species 2 were added to the system, the maximum-quality visits from the new pollinator could prevent the plant extinction, and thereby rescue the generalist pollinator.

The example in Fig. 5 only has two plant species (for clarity of illustration), but the plants' extinction risk becomes greater for larger number of plant species, particularly in overly connected networks (Valdovinos et al. 2016). In the simplest case where all plant species receive visits with

the same efficiency τ_{ij} and the plant abundances are at their (nearly identical) carrying capacities $p_i \approx 1/w$, the visit quality of a generalist pollinator species j (without adaptive foraging) is simply the inverse of the number of plant species P_j that it visits. A specialist plant species visited by pollinator species j alone can survive in these conditions only when $P_j < 1/\sigma_c$. In practice, specialist plant species require even lower levels of connectivity in their pollinator species (i.e., more specialized pollinators) if they are to avoid extinction, because rapid expansion of generalist plant populations during the transient dynamics dilutes the pollen of specialist plants even more than at equilibrium. In other words, the quality σ_{ij} is smaller than $1/P_j$ during the initial transient in a typical simulation.

4. *Effects of adaptive foraging*

As described above, the effect of the adaptive foraging dynamics contained in Eq. (4) is to rotate the ZNGIs and impact vectors in the direction of the more plentiful floral rewards. All the ZNGIs still pass through the coexistence point R_i^*, and adaptive foraging causes them to rotate about this point. In this section, we explain the consequences of this rotation for the survival of pollinators and plants in nested networks.

Fig. 7 shows how adaptive foraging changes the first result for pollinators illustrated in Fig. 5. In this example, the supply point lies just outside the coexistence cone, so the equilibrium state with fixed foraging preferences gives plant species 2 a higher equilibrium concentration of floral rewards. This means that the generalist pollinators will begin to focus their foraging efforts on plant species 2, resulting in a rotation of the ZNGI and impact vector to become more like those pollinators specialized on plant species 2 (i.e., a horizontal line and vertical arrow in this visualization). This rotation opens up the coexistence cone until it engulfs the supply point. When this happens, the resource abundances relax to the coexistence point (R_1^*, R_2^*), where both plants are equally good food sources, and adaptation stops.

Regarding the second result presented in Fig. 5, the equilibrium point is already at (R_1^*, R_2^*) even without adaptive foraging. This means that adaptation only takes place during the transient

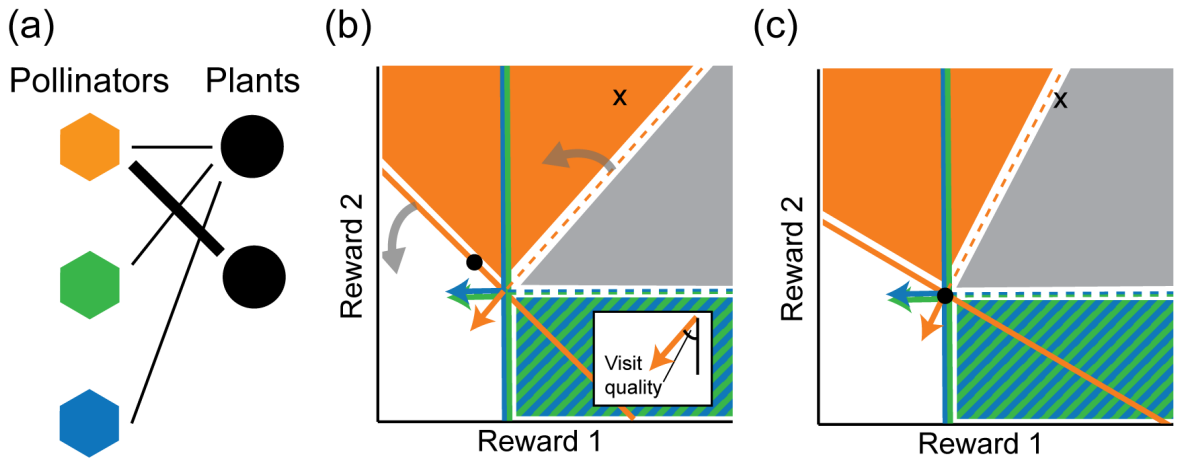

Figure 7: **Effects of adaptive foraging on pollinators.** *(a)* Illustration of nested network from previous examples, but with the addition of adaptive foraging, which allows the generalist pollinator species to focus its foraging effort on the plant species with more abundant floral rewards (thick line connecting first pollinator to second plant). *(b)* Since the equilibrium state of the nested network of Fig. (5) has more available rewards in plant species 2 than in species 1, adaptive foraging causes the ZNGI of the generalist pollinator species and its impact vector to rotate counterclockwise. The inset indicates how to extract from our graphical approach the visit quality of the generalist pollinator species (orange) to the specialist plant species (species 2), with larger angles corresponding to lower quality (see Fig. 3). *(c)* The rotation of the impact vector expands the coexistence cone, which now contains the supply point, so that all three species coexist in the new equilibrium. This also reduces the angle between the impact vector and the axis representing rewards from plant species 2, increasing the quality of visits by the generalist pollinators to these plants.

relaxation to equilibrium. In previous numerical simulations where all pollinator species are initialized with the same population size, however, adaptation still qualitatively tends in the same direction as in the first example (Fig. 7). This is because rewards of generalist plants are initially depleted to lower levels due to the higher total abundance of consumers from various pollinator species, causing the pollinators to shift their foraging efforts towards the specialist plant species.

The main effect of adaptive foraging on the dynamics of plant species is the modification of the visit quality σ_{ij}. In Fig. 3, we pointed out that σ_{ij} is related to the angle that the impact vector of species j makes with the rewards axis for plant species i. When the impact vector is parallel to the axis, the visit quality is perfect ($\sigma_{ij} = 1$), and the quality drops to zero as the impact vector becomes perpendicular to the axis. If the average quality of visits to a given plant is too low, the plant species no longer produces sufficient offspring to balance mortality. The species goes extinct, and the supply point for the rewards moves to zero along the corresponding rewards axis. For specialist plants, there is a simple expression for the minimum quality level σ_c required to avoid extinction, as discussed above and derived in Appendix C.

As noted above, adaptive foraging causes pollinator species to focus their foraging efforts on more specialist plant species. This entails an increase in the angle between the impact vector and the rewards axes of more generalist plant species, as illustrated in Fig. 8. The visit quality therefore decreases, and if it becomes too low, the generalist plant species will go extinct. This extinction process can happen whenever there is a generalist plant species that is not visited by any pure specialist pollinators, which explains the result found by extensive numerical simulations of adaptive foraging causing the extinction of generalist plant species in overly-connected networks (i.e., with many more interactions than the ones found in empirical networks, Valdovinos et al. 2016).

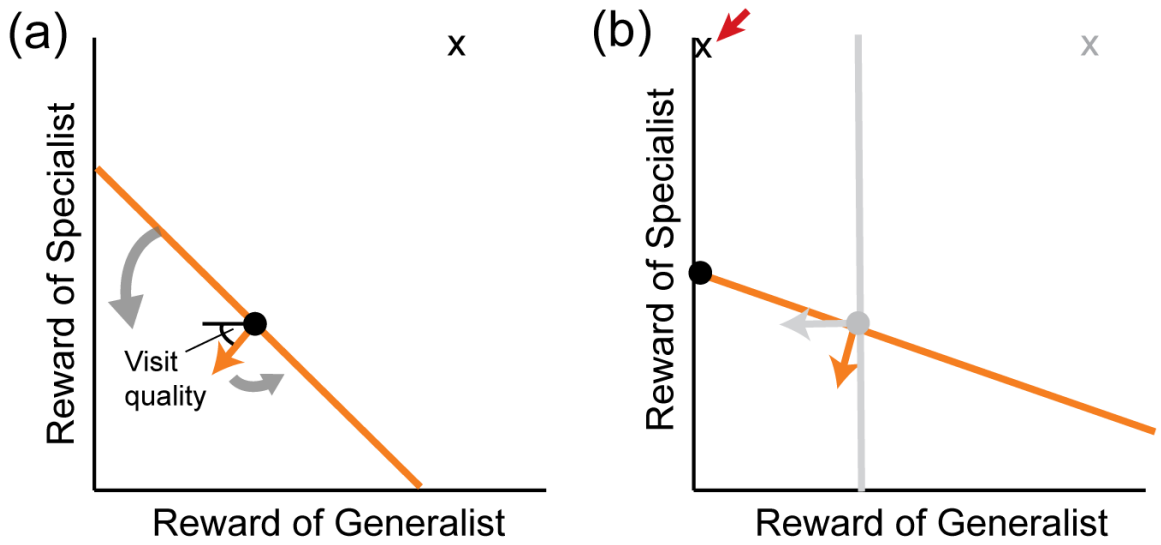

Figure 8: **Effects of adaptive foraging on plants.** *(a)* Adaptive foraging rotates impact vectors away from rewards axes corresponding to generalist plant species, whose rewards are rapidly depleted when the system is initialized with equal abundances of all pollinator species. The growing angle between the impact vector and the rewards axis of a generalist plant implies a reduction in visit quality for this plant species. *(b)* If the angles between the impact vectors and this axis become too large for all the pollinators servicing the generalist plant, the species goes extinct due to insufficient pollination. The supply point thus drops to zero along this axis, as highlighted by the red arrow. If the generalist species is visited by a purely specialist pollinator species (light gray ZNGI), however, the high quality visits from this species (impact vector parallel to the corresponding rewards axis) allows the generalist plant species to persist, and the supply point remains at the position of the gray 'x,' with both plant species supplying rewards.

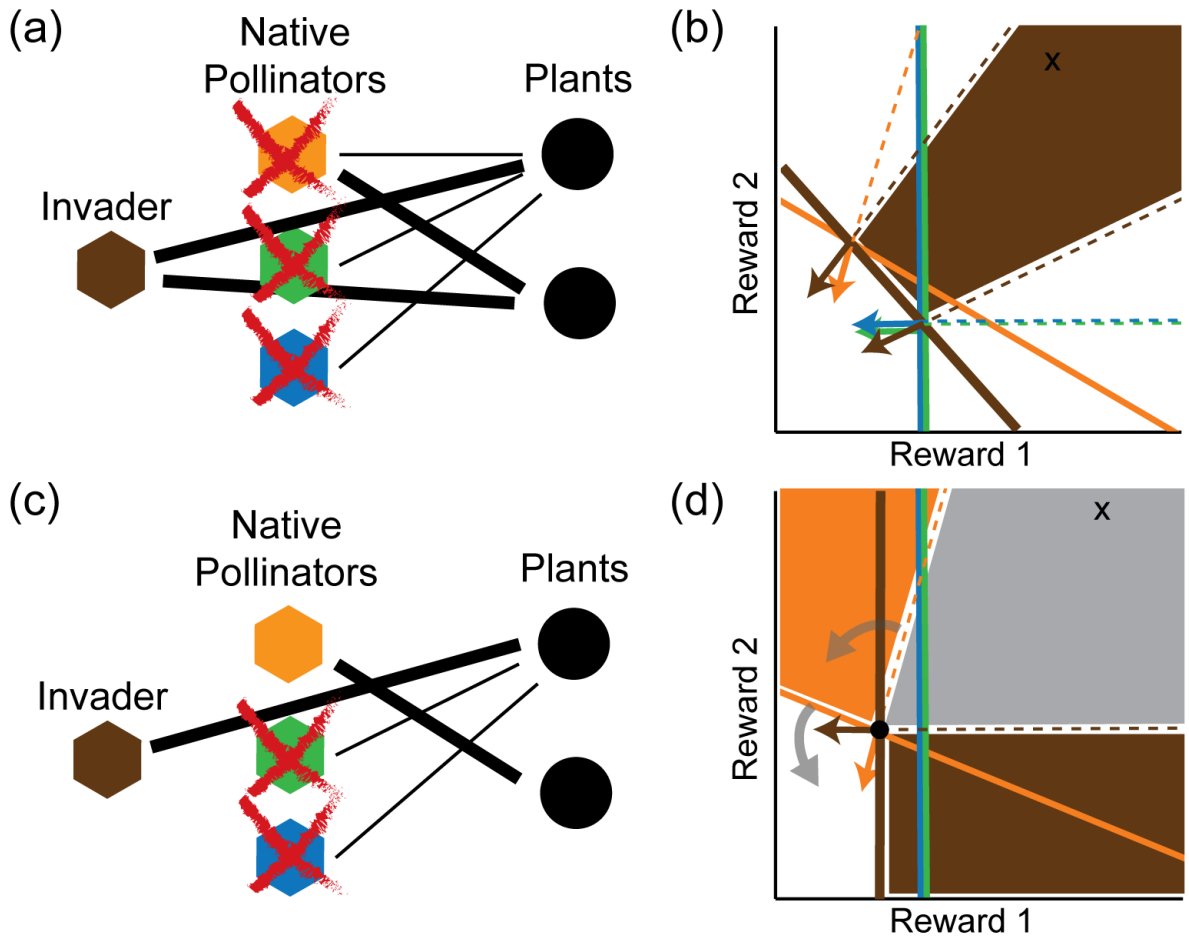

Figure 9: **Pollinator invasions.** *(a)* Brown polygon represents a generalist alien species with visit efficiency τ_{ij} greater than that of the three native species. *(b)* If all plant species have similar population sizes, as is the case of the numerical simulations in Valdovinos et al. (2018), the supply point in this scenario falls outside the coexistence cones, and only the invader survives at equilibrium. *(c)* Second scenario where the invader is a specialist pollinator species that does not interact with plant species 2. *(d)* The supply point now falls inside the coexistence cone with the orange native species. Since plant species 2 contains more rewards than species 1 at the coexistence point, adaptive foraging drives the native species to become a pure specialist on plant 2. As side effects, plant species 2 receives more effective pollination services and the native pollinator species reduces its population size. Plant extinctions do not occur under these conditions.

5. Impact of pollinator invasions on native species

Finally, we consider the consequences of invasions by new pollinator species from a different regional species pool. For our purposes, the essential characteristic of an invasive species is that its consumption and mortality rates do not follow the strict relationship imposed on the species within the focal species pool, and so its ZNGI does not necessarily pass through R_i^*.

If all the native species stably coexist, as in the first scenario of Fig. 5 or the adaptive foraging scenario of Fig. 7, the invader will establish whenever the native coexistence point R_i^* falls on the positive growth rate side of the invader's ZNGI. In the case of the numerical simulations by Valdovinos et al. (2018), this corresponded to the efficient alien species (i.e., with double the foraging efficiency τ_i of the native pollinator species). The new ZNGI alters the set of potential coexistence points, as illustrated in Fig. 9. In the case where native pollinator species share all their food sources (i.e., rewards) with the efficient invader, our two-plant three-pollinator native network allows two possible outcomes: either the invader coexists with the generalist, or it coexists with the specialists (Fig. 9*(b)*). But there is now a gap between the two coexistence cones. If the supply point falls in this gap, then only the invader survives, and all the native species go extinct. In the regime we have been considering here (i.e., all plant species have similar properties), the supply point will in fact typically fall into this gap and the only way for a native pollinator species to survive is to forage on plant species that the invader does not visit at all. Fig. 9*(c-d)* illustrates this case, with the invader now incapable of visiting plant 2. As a result, the invader now generically coexists with the generalist, and plant 2 has more usable rewards at the new coexistence point than plant species 1. This means that the native generalist will shift more and more of its foraging effort towards plant 2, until it becomes a pure specialist on that plant. Pollinator invasions do not cause plant extinctions, at least under the conditions studied here and in Valdovinos et al. (2018).

Discussion

Mutualistic systems sustain the productivity and biodiversity of most ecosystems in the planet (Thompson 1994; Peay 2016; Potts et al. 2016). Therefore, understanding the mechanisms by which their hundreds of species coexist is of major relevance for answering fundamental questions in ecology and also informing conservation efforts. Here, we advance understanding of species coexistence in mutualistic systems by expanding Contemporary Niche Theory to analyze the dynamics of plant-pollinator networks. In a nutshell, we found that all pollinator species observed in those networks are able to coexist if they require the same amount of rewards to balance out their reproduction and mortality rates, and that amount is provided by their mutualistic plants. In addition, we found that plant species can coexist as long as their intra-specific competition for resources other than pollination services is stronger than their competition with other plant species, and the quality of pollinator visits they receive is above a critical value whose exact expression for specialist plants we provided in Appendix C. Moreover, we showed that successfully accessing the floral rewards required by pollinators and the visit quality required by plants strongly depended on the network structure and adaptive foraging. Finally, we demonstrated that invasions by efficient pollinator species alter species coexistence causing the extinction of native pollinators or reducing their abundance.

Previous studies on species coexistence in plant-pollinator systems mainly consisted of work developing conceptual (e.g., Palmer et al. 2003; Mitchell et al. 2009) and mathematical (e.g., Levin and Anderson 1970; Johnson and Bronstein 2019), frameworks for analyzing conditions at which species can coexist, and reviews of empirical cases showing competition among plant species for pollination services (e.g., Mitchell et al. 2003, Morales and Traveset 2009) and among pollinator species for floral rewards (e.g., Palmer et al. 2003). The Contemporary Niche Theory allows a synthesis of all this information in one framework (see Methods) and makes quantitative predictions about community dynamics including species coexistence. Recently, Peay (2016) expanded this theory for mycorrhizal mutualisms, which allowed him to analyze the requirements for sur-

vival (requirement niche) and the impact on the environment (impact niche) of the interacting species, and to evaluate species coexistence. Our work further expands Contemporary Niche Theory of mutualistic interactions by incorporating plant-pollinator systems. We advance this theory by analyzing short- and long-term dynamics of plant-pollinator interactions, depicting the requirement and impact niches of pollinators, and demonstrating the effect of adaptive foraging and network structure on the pollinators' niches. In the following paragraphs, we explain each of these advances and contextualize them with previous literature.

Explicit consideration of two timescales: The Rewards and Plant Spaces

Explicit consideration of timescales has been recently highlighted as paramount for analyzing ecological systems, especially when evaluating management strategies (Callicott 2002; Hastings 2016) where the timeframe of action determines the ecological outcome. This is particularly the case of plant-pollinator systems whose dynamics can be distinctively divided into at least two timescales, the short-term dynamics occurring within a flowering season and the long-term dynamics occurring across flowering seasons (i.e., over years). We developed our graphical approach for these short- and long-term dynamics by representing the pollinators' niches in the Rewards and Plant Spaces, respectively. The Rewards Space depicts the rewards abundances of each plant species as the pollinators' niche axes, while the Plant Space represents these axes as the plant populations themselves. The former assumes approximately constant plant populations, analyzing the dynamics occurring during a flowering season where plants do not reproduce but produce floral rewards that are depleted by pollinators in a matter of hours or days. The Plant Space represents the longer time-scale at which the quality and quantity of pollinator visits impact plant populations represented on the axes.

As mentioned above, the other work we know that expands Contemporary Niche Theory to mutualisms was developed by Peay (2016). Peay explicitly models how mycorrhizal mutualism affects plant and fungal community dynamics in a more classic consumer-resource space, where the niche axes are the resources used by plant species. That is, that work shows how the ZNGIs

of plants change when the mycorrhizal mutualism is added, but the axes are still resources in the soil, not mutualists. In our work, by contrast, the axes are the abundances of the mutualistic partners themselves (plants) or the rewards produced by them (floral rewards).

Depicting the pollinators' requirement and impact niches

The requirement niche encapsulates an organism's requirements for survival (Leibold 1995). Here, we study the case in which pollinators only require floral rewards to survive. Thus, their requirement niches are depicted by the zero-net-growth isoclines (ZNGIs) that separate the region of rewards (or plant) abundances where the pollinators' growth rates are positive from the states where they are negative. Mathematically analyzing the requirement niche of species sharing resources has been long used to study species coexistence (MacArthur 1970; Tilman 1982; Leibold 1995; Chase and Leibold 2003). Only recently, however, these types of analyses have been applied to plant-pollinator systems. In particular, Johnson and Bronstein (2019) applied the R* Theory (Tilman 1982) to two pollinator species competing for the rewards provided by a shared plant species, and then to the same system but adding an abiotic resource (case not studied here).

Our results on the pollinators' requirement niche in rewards space without adaptive foraging are similar to the results obtained by Johnson and Bronstein (2019) in two ways. First, both studies find that two pollinator species can coexist when competing for floral rewards of one plant species only if they need the same amount of rewards for balancing out their mortality and reproduction rates. Second, both studies demonstrate that the competition outcome (pollinator coexistence, or extinction of one or both species) affects the plant population providing the rewards. Our analysis in plant space, however, further advances in this result by directly illustrating the positive impact of pollinator species on their mutualistic plants (see below). Moreover, by explicitly considering short- and long- term dynamics, our graphical approach clarifies one main difference between competition for resources within classic consumer-resource models and mutualistic interactions. In the classic case, consumers only negatively affect each other through depleting the shared resource, while in the mutualistic case consumers potentially benefit each

other through benefiting their shared mutualistic partner. Another difference between our work and the work by Johnson and Bronstein (2019) is that we extend our approach to mutualistic networks of any given number of plant and pollinator species, where the structure of interactions strongly affects the community dynamics (see below). On the down side, the model studied here – and therefore our approach – does not explicitly include other resource or abiotic limitations that pollinators or plants might require to survive (e.g., nesting sites, water), which should be addressed in future work.

The impact niche of an organism represents the magnitude and direction of change that the organism induces on its environment (Leibold 1995). In the case of pollinators studied here, their impact niche corresponds to the change they induce on rewards and plant abundances. In plant space, the mutualism is directly visible in the impacts, which represent the number of successful pollination events caused by each pollinator, and the impact vectors point in the direction of larger plant population sizes. In rewards space, the impact of a pollinator species is simply the rate at which it depletes the floral rewards, just as in a classic model of resource competition. An important difference to the classical case, however, is the representation of the visit quality of a particular pollinator species to a particular plant species in terms of the angle between the impact vector of the pollinator species and the rewards axis corresponding to the plant species.

Building off this novel representation of visit quality, we were able to advance another subject that has captured the attention of ecologists for over a century, that is, plant competition for pollination (reviewed in Mitchell et al. 2009). This large body of research has shown that plant species sharing the same pollinator species potentially compete not only for the pollinators' quantity of visits but also for their quality of visits. Our approach provides means for quantitatively analyzing these two aspects of plant competition for pollination and, therefore, moves beyond the previous empirical and conceptual approaches.

Demonstrating the effects of network structure and adaptive foraging on pollinators' niches

The network structure of plant-pollinator interactions determines which floral rewards are shared between any two given pollinator species and which pollinator species are shared between any two given plant species. Therefore, such network structure determines community dynamics and species coexistence. Here, we showed how our graphical approach accommodates the widely observed nested structure of plant-pollinator networks. More specifically, we were able to analyze the dynamics that occur in systems where generalist and specialist pollinators share the floral rewards of generalist plants, while specialist plants are visited only by generalist pollinators. Using our approach, we were able to verify results found by previous simulations (Valdovinos et al. 2013, 2016). That is, nestedness increases the niche overlap among pollinator species for floral rewards and among plant species for pollinators' visits, causing specialist species to go extinct. Regarding adaptive foraging, we found that this adaptive behavior causes the ZNGI's and impact vectors of pollinator species to rotate in the direction of the most abundant rewards, allowing for pollinator coexistence in nested networks through niche partitioning. Although these results were previously found by numerical simulations (Valdovinos et al. 2013, 2016), to our knowledge, this is the first time that the effects of network structure and adaptive foraging are incorporated in the Contemporary Niche Theory of mutualistic systems.

Conclusion

Our graphical approach advances Contemporary Niche Theory by incorporating network structure, adaptive foraging, quality of visits, and pollinator invasions. We identified a main difference between the purely competitive and the mutualistic niche, that is, the supply point for one guild (in our case plants or pollinators) is maintained by the activity of their mutualistic partners. We hope this research will promote development of ecological theory on mutualisms which is crucial for answering fundamental questions in ecology and also informing conservation efforts.

Acknowledgments

We thank George Kling for his comments on earlier versions of this manuscript.This research was funded by US NSF (DEB-1834497) to FSV.

Literature Cited

Abrams, P. 1987. On classifying interactions between populations. Oecologia 73:272.

Allesina, S., and S. Tang. 2012. Stability criteria for complex ecosystems. Nature 483:205.

Bascompte, J., and P. Jordano. 2007. Plant-animal mutualistic networks: the architecture of biodiversity. Annu. Rev. Ecol. Evol. Syst. 38:567.

———. 2014. Mutualistic networks. Princeton University Press, Princeton, NJ.

Bascompte, J., P. Jordano, C. J. Melián, and J. M. Olesen. 2003. The nested assembly of plant–animal mutualistic networks. Proceedings of the National Academy of Sciences 100:9383.

Bascompte, J., P. Jordano, and J. Olesen. 2006. Asymmetric coevolutionary networks facilitate biodiversity maintenance. Science 312:431.

Bastolla, U., M. Fortuna, A. Pascual-García, A. Ferrera, B. Luque, and J. Bascompte. 2009. The architecture of mutualistic networks minimizes competition and increases biodiversity. Nature 458:1018.

Boucher, D. 1985. Lotka-volterra models of mutualism and positive density-dependence. Ecol. Model. 27:251.

Boucher, D., S. James, and K. Keeler. 1982. The ecology of mutualism. Annual Review of Ecology and Systematics 13:315.

Bronstein, J. 2015. The study of mutualism. *In* J. Bronstein, ed., Mutualism. Oxford University Press, Oxford.

Brown, B. 1997. Coral bleaching: causes and consequences. Coral Reefs 16:S129.

Callicott, J. B. 2002. Choosing appropriate temporal and spatial scales for ecological restoration. Journal of Biosciences 27:409–420.

Chase, J. M., and M. A. Leibold. 2003. Ecological niches: linking classical and contemporary approaches. University of Chicago Press, Chicago, IL.

Chesson, P. 2000. Mechanisms of maintenance of species diversity. Annual review of Ecology and Systematics 31:343.

Czárán, T. L., R. F. Hoekstra, and L. Pagie. 2002. Chemical warfare between microbes promotes biodiversity. Proceedings of the National Academy of Sciences 99:786.

Elton, C. 1927. Animal Ecology. Sidgwick and Jackson, London, UK.

Gause, G. F., and A. A. Witt. 1935. Behavior of mixed populations and the problem of natural selection. The American Naturalist 69:596.

Goulson, D., E. Nicholls, C. Botías, and E. Rotheray. 2015. Bee declines driven by combined stress from parasites, pesticides, and lack of flowers. Science 347:1255957.

Hastings, A. 2016. Timescales and the management of ecological systems. Proceedings of the National Academy of Sciences 113:14568–14573.

Hogben, L., ed. 2013. Handbook of linear algebra. Chapman and Hall/CRC.

Holland, J., and D. DeAngelis. 2010. A consumer-resource approach to the density-dependent population dynamics of mutualism. Ecology 91:1286.

Holland, J., J. Ness, A. Boyle, and J. Bronstein. 2005. Mutualisms as consumer-resource interactions. Ecology of predator–prey interactions page 17.

Holling, C. S. 1959. Some characteristics of simple types of predation and parasitism. The Canadian Entomologist 91:385.

Horton, T., and T. Bruns. 2001. The molecular revolution in ectomycorrhizal ecology: peeking into the blackbox. Mol. Ecol. 10:1855.

Huisman, J., and F. Weissing. 1999. Biodiversity of plankton by species oscillation and chaos. Nature 402:407.

Hutchinson, G. E. 1957. Concluding remarks. Cold Spring Harbor Symposium on Quantitative Biology .

———. 1961. The paradox of the plankton. The American Naturalist 95:137–145.

Johnson, C., and J. Bronstein. 2019. Coexistence and competitive exclusion in mutualism. Ecology 100:e02708.

Kelsic, E. D., J. Zhao, K. Vetsigian, and R. Kishony. 2015. Counteraction of antibiotic production and degradation stabilizes microbial communities. Nature 521:516.

Kerr, B., M. A. Riley, M. W. Feldman, and B. J. Bohannan. 2002. Local dispersal promotes biodiversity in a real-life game of rock–paper–scissors. Nature 418:171.

Koffel, T., T. Daufresne, F. Massol, and C. A. Klausmeier. 2016. Geometrical envelopes: Extending graphical contemporary niche theory to communities and eco-evolutionary dynamics. Journal of Theoretical Biology 407:271.

Kostitzin, V. 1934. Symbiose, Parasitisme et Evolution (Etude Mathematique). Hermann et Cie, Paris.

Leibold, M. A. 1995. The niche concept revisited: mechanistic models and community context. Ecology 76:1371–1382.

———. 1998. Similarity and local co-existence of species in regional biotas. Evolutionary Ecology 12:95.

Levin, D. A., and W. W. Anderson. 1970. Competition for pollinators between simultaneously flowering species. The American Naturalist 104:455–467.

Levin, S. 1974. Dispersion and population interactions. The American Naturalist 108:207.

Levin, S. A. 1970. Community equilibria and stability, and an extension of the competitive exclusion principle. The American Naturalist 104:413.

Levins, R. 1979. Coexistence in a variable environment. The American Naturalist 114:765.

MacArthur, R. 1969. Species packing, and what competition minimizes. Proceedings of the National Academy of Sciences 64:1369.

———. 1970. Species packing and competitive equilibrium for many species. Theoretical population biology 1:1–11.

McGehee, R., and R. A. Armstrong. 1977. Some Mathematical Problems Concerning the Ecological Principle of Competitive Exclusion. Journal of Differential Equations 23:30.

Mitchell, R. J., R. J. Flanagan, B. J. Brown, N. M. Waser, and J. D. Karron. 2009. New frontiers in competition for pollination. Annals of Botany 103:1403–1413.

Morales, C. L., and A. Traveset. 2009. A meta-analysis of impacts of alien vs. native plants on pollinator visitation and reproductive success of co-flowering native plants. Ecology Letters 12:716–728.

Okuyama, T., and J. Holland. 2008. Network structural properties mediate the stability of mutualistic communities. Ecol. Lett. 11:208.

Ollerton, J. 2017. Pollinator diversity: distribution, ecological function, and conservation. Annu. Rev. Ecol. Evol. Syst. 48:353.

Ollerton, J., R. Winfree, and S. Tarrant. 2011. How many flowering plants are pollinated by animals? Oikos 120:321.

Pacciani-Mori, L., A. Giometto, S. Suweis, and A. Maritan. 2019. Adaptive metabolic strategies in consumer-resource models. bioRxiv 10.1101/385724.

Palmer, T. M., M. L. Stanton, and T. P. Young. 2003. Competition and coexistence: exploring mechanisms that restrict and maintain diversity within mutualist guilds. The American Naturalist 162:S63–S79.

Peay, K. 2016. The mutualistic niche: Mycorrhizal symbiosis and community dynamics. Annu. Rev. Ecol. Evol. Syst. 47:143.

Posfai, A., T. Taillefumier, and N. Wingreen. 2017. Metabolic trade-offs promote diversity in a model ecosystem. Physical Review Letters 118:028103.

Potts, S., V. Imperatriz-Fonseca, H. Ngo, M. Aizen, J. Biesmeijer, and T. Breeze. 2016. Safeguarding pollinators and their values to human well-being. Nature 540:220.

Richerson, P., R. Armstrong, and C. R. Goldman. 1970. Contemporaneous disequilibrium, a new hypothesis to explain the 'paradox of the plankton'. Proceedings of the National Academy of Sciences 67:1710.

Rowan, R. 2004. Coral bleaching: thermal adaptation in reef coral symbionts. Nature 430:742.

Thompson, J. N. 1994. The coevolutionary process. University of Chicago Press.

Tilman, D. 1982. Resource competition and community structure, vol. 17. Princeton University Press.

Turner, P. E., V. Souza, and R. E. Lenski. 1996. Tests of ecological mechanisms promoting the stable coexistence of two bacterial genotypes. Ecology 77:2119.

Valdovinos, F. S. 2019. Mutualistic networks: moving closer to a predictive theory. Ecology Letters 22:1517.

Valdovinos, F. S., E. L. Berlow, P. M. De Espanés, R. Ramos-Jiliberto, D. P. Vázquez, and N. D. Martinez. 2018. Species traits and network structure predict the success and impacts of pollinator invasions. Nature Communications 9:2153.

Valdovinos, F. S., B. J. Brosi, H. M. Briggs, P. Moisset de Espanés, R. Ramos-Jiliberto, and N. D. Martinez. 2016. Niche partitioning due to adaptive foraging reverses effects of nestedness and connectance on pollination network stability. Ecology Letters 19:1277.

Valdovinos, F. S., P. Moisset de Espanés, J. D. Flores, and R. Ramos-Jiliberto. 2013. Adaptive foraging allows the maintenance of biodiversity of pollination networks. Oikos 122:907.

van der Heijden, M., R. Bardgett, and N. van Straalen. 2008. The unseen majority: soil microbes as drivers of plant diversity and productivity in terrestrial ecosystems. Ecology Letters 11:296.

Vandermeer, and Boucher. 1978. Varieties of mutualistic interaction in population models. J. Theor. Biol. 74:549.

Vázquez, D. P., N. Blüthgen, L. Cagnolo, and N. P. Chacoff. 2009. Uniting pattern and process in plant–animal mutualistic networks: a review. Annals of Botany 103:1445.

Wang, B., and T. Smith. 2002. Closing the seed dispersal loop. Trends in Ecology & Evolution 17:379.

Wolin, C., and L. Lawlor. 1984. Models of facultative mutualism: Density effects. The American Naturalist 124:843.

Xue, C., and N. Goldenfeld. 2017. Coevolution maintains diversity in the stochastic 'kill the winner' model. Physical Review Letters 119:268101.

Yodzis, P., and S. Innes. 1992. Body size and consumer-resource dynamics. The American Naturalist 139:1151.

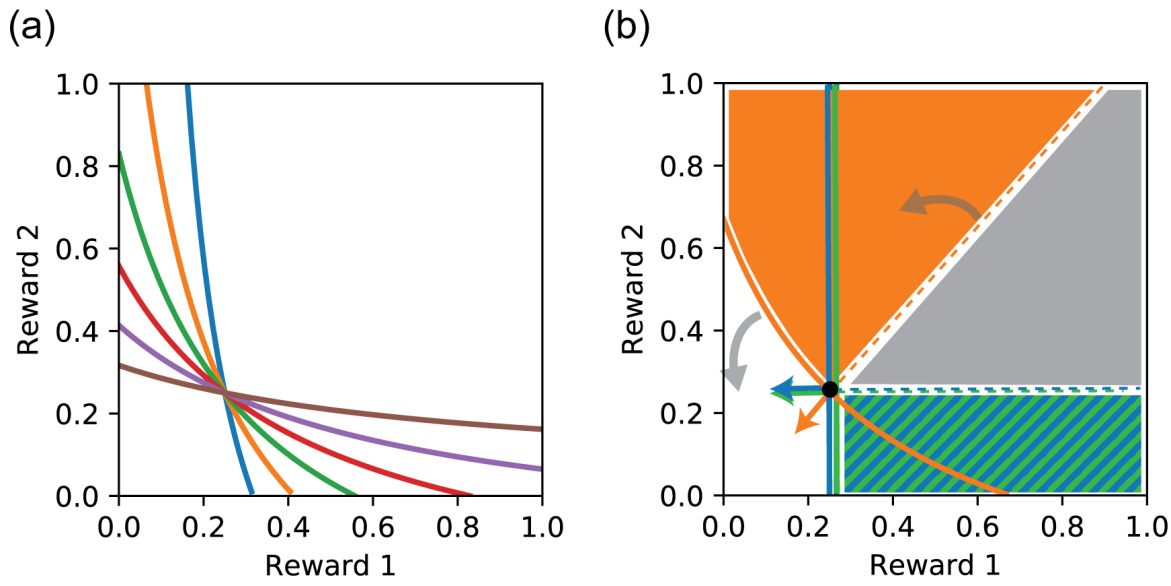

Figure A1: **Saturating growth laws.** *(a)* Scaling the maximum mass-specific rewards uptake rate with the pollinator mortality rate ensures that all ZNGIs cross in models with saturating growth kinetics, just as in the original linear model. *(b)* ZNGIs, impact vectors, supply vector and coexistence cone for the nested network of Fig. 5, with saturating rewards uptake following Eq. (A1). Gray arrows indicate the direction of rotation of the ZNGI and coexistence cone boundary under adaptive foraging.

Appendix A: Saturating functional responses

In the version of the model presented in the main text, which was employed in all the simulations, the pollinator growth rates are linear functions of reward abundances. In reality, both the quantity of rewards extracted per visit f_{ij} and the visit frequency V_{ij} are likely to saturate at high rewards levels. All the qualitative results obtained in the main text apply to these more realistic models as well, with a slight modification of the assumptions about parameter correlations. In this Appendix, we provide mathematical expressions for these two types of saturation, along with the assumptions required to ensure that all ZNGIs intersect as in Fig. 4*(a)*.

The original publication presenting the model (Valdovinos et al. 2013) contained a discussion of saturating rewards extraction, with each pollinator capable of obtaining a finite quantity $b_{ij}^{\max}$

of rewards per visit, following Holling's Type II growth kinetics (Holling 1959):

$$f_{ij} = b_{ij}^{\max} \frac{R_i}{\kappa_{ij} p_i + R_i}. \tag{A1}$$

Setting $da_j/dt = 0$ in Eq. 3, we can obtain the equation for the ZNGIs and find that they all intersect at a point R_i^* when

$$c_{ij} \tau_{ij} b_{ij}^{\max} = \mu_j^A \frac{\kappa_i p_i + R_i^*}{p_i R_i^*} \tag{A2}$$

with saturation constants κ_i independent of j. As long as the maximum mass-specific rewards uptake rate $c_{ij}\tau_{ij}b_{ij}^{\max}$ is proportional to the mortality rate μ_j^A for all pollinator species j visiting a given plant species i, one can always find a set of reward abundances R_i^* that satisfy this equation.

In addition to the finite capacity of a pollinator to extract rewards on each visit, it is reasonable to assume that there is a maximum number of visits that an animal can make per unit time. Using the same Type II kinetics, we obtain the following expression for the total visitation rate of pollinator species j on plant species i:

$$V_{ij} = a_j \frac{\tau_{ij} \alpha_{ij} p_i}{1 + \sum_k \tau_{kj} \alpha_{kj} h_{kj} p_k + \sum_k \omega_{jk} a_k}. \tag{A3}$$

Here h_{kj} is the handling time for pollinator species j foraging on plant species k, and ω_{jk} quantifies the magnitude of direct interference between pollinators. Direct interference significantly complicates the geometric interpretation, so we will set $\omega_{jk} = 0$ here. As noted in the main text, however, nonzero ω_{jj} provides a simple mechanism for CEP violation, and is of interest for future study. If the saturation of visit frequency is the only relevant nonlinearity, and the rewards uptake per visit is still linear in R_i, then the ZNGIs remain linear. When both kinds of saturation are present, the intersection point R_i^* is defined by:

$$c_{ij} \tau_{ij} b_{ij}^{\max} = \mu_j^A \frac{(\kappa_i p_i + R_i^*)(1 + \sum_k \tau_{kj} \alpha_{kj} h_{kj} p_k)}{p_i R_i^*}. \tag{A4}$$

Simultaneously satisfying this equation for an arbitrary number of pollinator species j requires the additional assumptions that the handling time h_{kj} is inversely proportional to the visitation efficiency τ_{kj} for all pollinator species j visiting a given plant species k, and that all the plant

population densities (for non-extinct plants) are the same. Both of these are trivially satisfied under conditions similar to the simulations discussed in the main text, where the only differences between species come from the topology of the interaction network, and all other parameters are species-independent.

Fig. A1 shows that the ZNGIs are no longer linear under saturating rewards extraction, but that the graphical arguments from the main text still hold. The key point is that when all parameters are species-independent (except for interaction network topology) the initial impact vectors are required by symmetry to be perpendicular to the ZNGIs, and adaptive foraging tends to rotate them away from the rewards axes corresponding to generalist plants, just as in the linear model. Since these are the two essential features necessary for recovering the simulation results, we expect that the same phenomena will be observed even in the presence of saturation.

Appendix B: Equilibrium of plant dynamics

In this appendix, we discuss the equilibrium state of the plant dynamics, in support of Fig. 4*(b)*. First, we consider the case of zero plant mortality ($\mu_i^P = 0$ for all i). From Eq. (1), we see that the equilibrium condition $dp_i/dt = 0$ reduces to $\gamma_i = 0$, that is:

$$0 = g_i(1 - \sum_{l \neq i \in P} u_l p_l - w_i p_i). \tag{A5}$$

This is a set of P linear equations in P unknowns, which generically has a single solution. We focus on the case of uniform parameters where $u_i = u$ and $w_i = w$ for all i. Then the solution is simply

$$p_i^* = \frac{1}{w + (P-1)u} \tag{A6}$$

for all plant species i. In two dimensions, we can visualize this solution as the point of intersection between the two lines $0 = 1 - up_2 - wp_1$ and $0 = 1 - up_1 - wp_2$, as shown in Fig. 4.

We now turn to nonzero mortality. It will be convenient to define the relative mortality

$$\tilde{\mu}_i^P = \frac{\mu_i^P}{g_i \sum_{j \in A_i} e_{ij}\sigma_{ij}\alpha_{ij}\tau_{ij}a_j} \tag{A7}$$

which is the ratio of the mortality rate to the production rate of new seedlings at low plant density ($\gamma_i = g_i$). In terms of this quantity, the equilibrium condition becomes

$$0 = 1 - \sum_{l \neq i \in P} u_l p_l - w_i p_i - \tilde{\mu}_i^P. \tag{A8}$$

The solutions to this equation for different values of $\tilde{\mu}_i^P$ sweep out the entire space defined by

$$0 \leq 1 - \sum_{l \neq i \in P} u_l p_l - w_i p_i \tag{A9}$$

This region is illustrated for the two-dimensional example in Fig. 4*(b)*, for a range of relative values of u and w. Equation (A8) also indicates that the zero-mortality solution with $\gamma_i = g_i(1 - \sum_{l \neq i \in P} u_l p_l - w_i p_i) = 0$ should be a good approximation whenever $\tilde{\mu}_i^P \ll 1$.

Finally, we can determine the stability of the fixed points by computing the eigenvalues of the Jacobian matrix

$$J_{ki} = \frac{\partial}{\partial p_k} \frac{dp_i}{dt} = \frac{\partial \gamma_i}{\partial p_k} \sum_{j \in A_i} e_{ij} \sigma_{ij} V_{ij} + \gamma_i \frac{\partial}{\partial p_k} \sum_{j \in A_i} e_{ij} \sigma_{ij} V_{ij} - \mu_i \delta_{ki}, \tag{A10}$$

evaluated at the equilibrium point p_i^*. To simplify the calculation, we assume a separation of timescales, as discussed in the main text, where the plant populations change slowly over many flowering seasons, while the rewards and animal populations relax quickly to a conditional equilibrium $a_j^*(p_k)$, given the current values of the plant abundances. We also assume that $w_i = w$ for all i and $u_l = u$ for all l. Evaluating the derivatives, we find:

$$J_{ki} = -\left(g_i \sum_{j \in A_i} e_{ij} \sigma_{ij} V_{ij} \right) [(w - u)\delta_{ki} + u] + \gamma_i \sum_{j \in A_i} e_{ij} \sigma_{ij} \alpha_{ij} \tau_{ij} p_i^* \frac{\partial a_j^*}{\partial p_k} + \left(\gamma_i \sum_{j \in A_i} e_{ij} \sigma_{ij} \alpha_{ij} \tau_{ij} a_j^* - \mu_i \right) \delta_{ki}. \tag{A11}$$

The final term in parentheses is equal to $d \log p_i / dt$ for $p_i > 0$, and so it must vanish whenever all the plants coexist. To determine the sign of the eigenvalues for the remaining portion, it is convenient to define the diagonal matrix $\mathbf{D}$ with components

$$D_{ki} = \delta_{ki} g_i \sum_{j \in A_i} e_{ij} \sigma_{ij} V_{ij} \tag{A12}$$

and a matrix $\mathbf{A}$ with components

$$A_{ki} = \frac{\gamma_i \sum_{j \in A_i} e_{ij}\sigma_{ij}\alpha_{ij}\tau_{ij}p_i^* \frac{\partial a_j^*}{\partial p_k}}{g_i \sum_{j \in A_i} e_{ij}\sigma_{ij}V_{ij}}. \tag{A13}$$

We can now write the Jacobian $\mathbf{J}$ in matrix notation as

$$\mathbf{J} = -\mathbf{D}[(w-u)\mathbf{I} + \mathbf{U} - \mathbf{A}] \tag{A14}$$

where $\mathbf{I}$ is the identity matrix and $\mathbf{U}$ is a matrix with elements $U_{ij} = u$.

In the low mortality limit $\tilde{\mu}_i^P \to 0$, where the coexistence point lies at the far corner of the space of allowed plant populations, we have $\gamma_i \to 0$ (as indicated above), and so $\mathbf{A} \to 0$. In this case, the eigenvalues of $[(w-u)\mathbf{I} + \mathbf{U}]$ can be evaluated exactly, with one eigenvalue equal to

$$\lambda^+ = w + (P-1)u \tag{A15}$$

and the rest equal to

$$\lambda^- = w - u. \tag{A16}$$

Standard results on D-stability can be used to show that multiplying $[(w-u)\mathbf{I} + \mathbf{U}]$ by a positive diagonal matrix $\mathbf{D}$ leaves the stability of the matrix unchanged, with the result that the eigenvalues of $\mathbf{J}$ are all negative if and only if $\lambda^- > 0$ (Hogben 2013). Thus we recover the classic result of modern coexistence theory: stable coexistence requires that intra-specific competition (w) is stronger than inter-specific competition (u) (Chesson 2000).

To determine the impact of nonzero $\mathbf{A}$, we focus on the case where all pollinators are pure specialists, with identical parameters. Then $\mathbf{A}$ is proportional to the identity matrix:

$$\mathbf{A} = \frac{1 - [(P-1)u + w]p^*}{a^*} \frac{\partial a^*}{\partial p} \mathbf{I} \tag{A17}$$

where $p_i^* = p^*$ and $a_j^* = a^*$ for all i and j, since all the parameters are the same. Since the pollinators feed on the rewards produced by the plants, $\partial a^*/\partial p$ is always positive. The smallest eigenvalue of $[(w-u)\mathbf{I} + \mathbf{U} - \mathbf{A}]$ becomes

$$\lambda^- = \tilde{w} - u \tag{A18}$$

where the effective intra-specific competition coefficient $\tilde{w}$ is

$$\tilde{w} = w - \frac{1 - [(P-1)u + w]p^*}{a^*} \frac{\partial a^*}{\partial p} \tag{A19}$$

which is always less than w. This means that the low-mortality criterion $w > u$ remains a necessary condition for coexistence. We conjecture that this remains true for arbitrary pollinator parameters and connectivity, because it there is no obvious reason why competition between different species of pollinators should selectively provide additional intra-specific feedback for the plants.

Appendix C: Plant extinction

We consider the equilibrium condition for a specialist plant of species i, which is visited by just one pollinator species j, obtained from Eq. (1) by substituting in for γ_i and V_{ij} using the linear model described in the main text:

$$0 = g_i(1 - w_i p_i) e_{ij} \sigma_{ij} \tau_{ij} \alpha_{ij} a_j - \mu_i^P. \tag{A20}$$

The pollinator population density a_j can be found by solving the equilibrium condition for the rewards, obtained from Eq. (2):

$$0 = \beta_i p_i - \phi_i R_i - b_{ij} \tau_{ij} \alpha_{ij} a_j R_i. \tag{A21}$$

To solve this, we recall that in the equilibrium state of interest, where all pollinators coexist, the reward abundances are equal to R_i^*. Thus we arrive at:

$$a_j = \frac{\beta_i p_i - \phi_i R_i^*}{b_{ij} \tau_{ij} \alpha_{ij} R_i^*}. \tag{A22}$$

Substituting in to the equilibrium condition for the plants, we have:

$$0 = g_i(1 - w_i p_i) e_{ij} \sigma_{ij} \frac{\beta_i p_i - \phi_i R_i^*}{b_{ij} R_i^*} - \mu_i^P. \tag{A23}$$

This is a quadratic equation in p_i, which can be solved to obtain:

$$p_i = \frac{1}{w_i} \left[1 - \frac{1}{2} (1 - d_i) \left(1 - \sqrt{1 - \frac{4}{s_{ij} \sigma_{ij} (1 - d_i)}} \right) \right] \tag{A24}$$

where

$$d_i = \frac{\phi_i R_i^* w_i}{\beta_i} \tag{A25}$$

is the fraction of floral rewards that are lost to dilution when the plant population is at its carrying capacity $1/w_i$, and

$$s_{ij} = \frac{g_i e_{ij} \beta_i (1 - d_i)}{w_i \mu_i^P b_{ij} R_i^*} \tag{A26}$$

is the number of seedlings produced per plant lifetime under optimal conditions, where there are no other plant species nearby to contaminate the pollen, and the field is kept clear of all competing plants. ($g_i e_{ij}$ is the number of individual seedlings produced per pollinator visit, $(1 - d_i)\beta_i/(\mu_i^P w_i)$ is the harvested rewards mass per unit area over the plant's lifetime, and $b_{ij} R_i^*$ is the rewards mass density harvested per visit).